ANESTHESIOLOGY

Information Integration and Mesoscopic Cortical Connectivity during Propofol Anesthesia

Zhenhu Liang, Ph.D., Lei Cheng, M.S., Shuai Shao, M.S., Xing Jin, M.S., Tao Yu, M.D., Jamie W. Sleigh, M.D., Xiaoli Li, Ph.D.

ANESTHESIOLOGY 2020; 132:504–24

EDITOR'S PERSPECTIVE

What We Already Know about This Topic

- Coupling of neuronal oscillations between brain regions is correlated with higher level brain activity
- Permutation cross mutual information can be used to evaluate information integration in the electroencephalogram during anesthesia.

What This Article Tells Us That Is New

- Using electrocorticography in subjects anesthetized with propofol, the genuine permutation cross mutual information demonstrated that, with loss of consciousness, there was a loss of efficient global information transmission and increased local functional segregation in the cortical network

ABSTRACT

Background: The neurophysiologic mechanisms of propofol-induced loss of consciousness have been studied in detail at the macro (scalp electroencephalogram) and micro (spiking or local field potential) scales. However, the changes in information integration and cortical connectivity during propofol anesthesia at the mesoscopic level (the cortical scale) are less clear.

Methods: The authors analyzed electrocorticogram data recorded from surgical patients during propofol-induced unconsciousness (n = 9). A new information measure, genuine permutation cross mutual information, was used to analyze how electrocorticogram cross-electrode coupling changed with electrode-distances in different brain areas (within the frontal, parietal, and temporal regions, as well as between the temporal and parietal regions). The changes in cortical networks during anesthesia—at nodal and global levels—were investigated using clustering coefficient, path length, and nodal efficiency measures.

Results: In all cortical regions, and in both wakeful and unconscious states (early and late), the genuine permutation cross mutual information and the percentage of genuine connections decreased with increasing distance, especially up to about 3 cm. The nodal cortical network metrics (the nodal clustering coefficients and nodal efficiency) decreased from wakefulness to unconscious state in the cortical regions we analyzed. In contrast, the global cortical network metrics slightly increased in the early unconscious state (the time span from loss of consciousness to 200 s after loss of consciousness), as compared with wakefulness (normalized average clustering coefficient: 1.05 ± 0.01 *vs.* 1.06 ± 0.03, $P = 0.037$; normalized average path length: 1.02 ± 0.01 *vs.* 1.04 ± 0.01, $P = 0.021$).

Conclusions: The genuine permutation cross mutual information reflected propofol-induced coupling changes measured at a cortical scale. Loss of consciousness was associated with a redistribution of the pattern of information integration; losing efficient global information transmission capacity but increasing local functional segregation in the cortical network.

(ANESTHESIOLOGY 2020; 132:504–24)

General anesthesia includes a reversible, drug-controlled loss of consciousness. It provides an effective way to study the neurophysiologic mechanisms of consciousness. However, because of the complexity of anesthetic effects on the central nervous system, a robust causal theory has yet to be established.

The information integration theory of consciousness is one contender. It has been shown that the coupling of neuronal oscillations between different frequency bands or regions can be correlated with high-level brain activity, such as sensory, motor, and cognitive events.[1,2] Alternatively, we may regard the brain as a complex system, and assess information integration by broadband information theory measures, such as entropy, complexity, and mutual information.[3–6] Compared with neural oscillation measures, evaluations of the information integration using entropy, complexity, and mutual information robustly capture the nonlinear coupling characteristics of neurophysiologic signals.[7]

Unfortunately, neurophysiologic data, such as electroencephalogram and local field potentials, are complex signals lacking clear and invariant signatures across unconscious states.[8] Symbolic analysis, as proposed by Bandt and Pompe,[9] is thought to be a simple but effective solution

This article is featured in "This Month in Anesthesiology," page 1A. Supplemental Digital Content is available for this article. Direct URL citations appear in the printed text and are available in both the HTML and PDF versions of this article. Links to the digital files are provided in the HTML text of this article on the Journal's Web site (www.anesthesiology.org). This article has a video abstract.

Submitted for publication February 4, 2018. Accepted for publication September 3, 2019. Published online first on November 6, 2019. From the Institute of Electrical Engineering, Yanshan University, Qinhuangdao, P.R. China (Z.L., L.C., S.S., X.J.); Beijing Institute of Functional Neurosurgery, Xuanwu Hospital, Capital Medical University, Beijing, P.R. China (T.Y.); Department of Anesthesia, Waikato Hospital, Hamilton, New Zealand (J.W.S.); State Key Laboratory of Cognitive Neuroscience and Learning and International Data Group/McGovern Institute for Brain Research, Beijing Normal University, Beijing, P.R. China (X.L.).

 Anesthesiology 2020; 132:504–24. DOI: 10.1097/ALN.0000000000003015

to this problem. As permutation patterns arise naturally in time series, rather than using amplitudes of signals the symbolization technique is a powerful alternative to quantify the information content of time series.[10,11] Because of these advantages, various permutation measures, such as permutation entropy, symbolic transfer entropy, weighted symbolic mutual information, and permutation cross mutual information, have been widely used in neurologic disease diagnosis and brain state monitoring,[12–16] especially for level of consciousness assessment.[7,8,15–18] Our previous studies[7,16] found that the permutation cross mutual information measure performed better in evaluating the information integration of prefrontal regions from electroencephalogram recordings for patients under propofol, or isoflurane and remifentanil, anesthesia.

Most of the works mentioned above only considered neural activity at the macro (scalp electroencephalogram) scale; investigations focused at the scale of cortical dynamical observations have been rare.[19] It is well known that the amounts of long-distance communication and information sharing between brain areas are important criteria for the evaluation of consciousness,[15,20–22] but how best to assess information integration at different spatial scales remains an open problem. This question motivated us to explore whether the permutation cross mutual information value could be used to estimate neural information integration at the mesoscale of electrocorticogram recordings, and to investigate information integration at different spatial distances.

Previous studies[23,24] have proposed a surrogate analysis method to estimate the genuine correlation strengths for multi-channel electroencephalogram. By correcting for spurious statistical correlations, we therefore propose a new genuine mutual information measure—the genuine permutation cross mutual information—which combines the permutation cross mutual information and surrogate analysis. Additionally, independent component analysis is used to solve the problems arising from volume conduction effects.[25,26] We use graph theory to measure network characteristics at the cortical scale. To investigate how information integration correlates with interelectrode distance, brain area, and state of anesthesia, we applied our methods to data from nine patients with epilepsy who were undergoing propofol anesthesia.

Materials and Methods

Data Recordings and Preprocessing

We recorded the electrocorticogram signals from nine patients (aged 18 to 54 yr) undergoing intracranial monitoring for surgical treatment of epilepsy at Xuanwu Hospital, Beijing, China. The recordings were done from March 1, 2012 to December 31, 2013. Patient information and electrode arrangements are presented in Supplemental Digital Content 1 (http://links.lww.com/ALN/C70). Patients were classified as American Society of Anesthesiologists Physical Status II or III. Patients provided written informed consent, and the protocol was approved by the Xuanwu Hospital ethics committee.

Sixty-four–channel electrocorticogram data were recorded during the transition from awake to unconscious states during predominantly propofol-induced general anesthesia before planned neurosurgery to remove the electrodes from the patients. The electrocorticogram data were recorded using a video-electroencephalogram monitoring system (DaVinci; USA). The monitoring system had a sampling rate of 256 Hz and the electrocorticogram data were prefiltered through a 0.15-Hz high-pass filter and a 67-Hz low-pass filter. The reference electrode and ground electrode were fixed under the scalp and the right shoulder, respectively. Loss of consciousness time point was determined every 5 s by loss of response to verbal commands.

Recordings were obtained in the operating room environment, which was not muted. The patients could blink or open and close their eyes before drug induction. Dosages of anesthetics were determined according to standard dosing requirements. The intravenous induction drugs were imidazole (0.1 mg/kg), fentanyl (2–4 μg/kg), vecuronium (0.1 mg/kg), and propofol (1–2 mg/kg).

Data were recorded for off-line analysis in MATLAB (version 2014, MathWorks Inc., USA). Line noise (50 Hz) was removed with an adaptive notch filter. Large amplitude electrocorticogram artifacts were removed and bad channels were rejected by visual inspection. A band-pass filter based on the EEGLAB function *eegfilt.m* was used to extract electrocorticogram data from 0.15 Hz to 45 Hz for index calculation. To maintain consistency with our previous study,[16] the electrocorticogram recordings were resampled to 100 Hz by running the *resample.m* function from MATLAB. One patient who had abundant motion noise and bad channels was excluded. The remaining eight patients were included in the analysis, seven of whom had 64-channel data, whereas one had 48-channel data.

Genuine Permutation Cross Mutual Information

Propofol-induced general anesthesia causes large low frequency oscillations. Because these low frequency oscillations in a finite dataset could have produced large spurious mutual information values,[24] we used surrogate techniques to measure the genuine coupling of pairs of electrocorticogram channels.[23,27] Diagrams of the analysis process and resulting genuine permutation cross mutual information and genuine cortical networks found by genuine permutation cross mutual information are shown in figure 1.

The details of the genuine permutation cross mutual information algorithm are as follows:

(1) Given two time series of x_t and y_t $t = 1,2,\ldots n$, a phase space reconstruction procedure was applied to construct the vectors $X_t[x_t, x_{t+\tau}, \ldots, x_{t+m\tau}]$ and

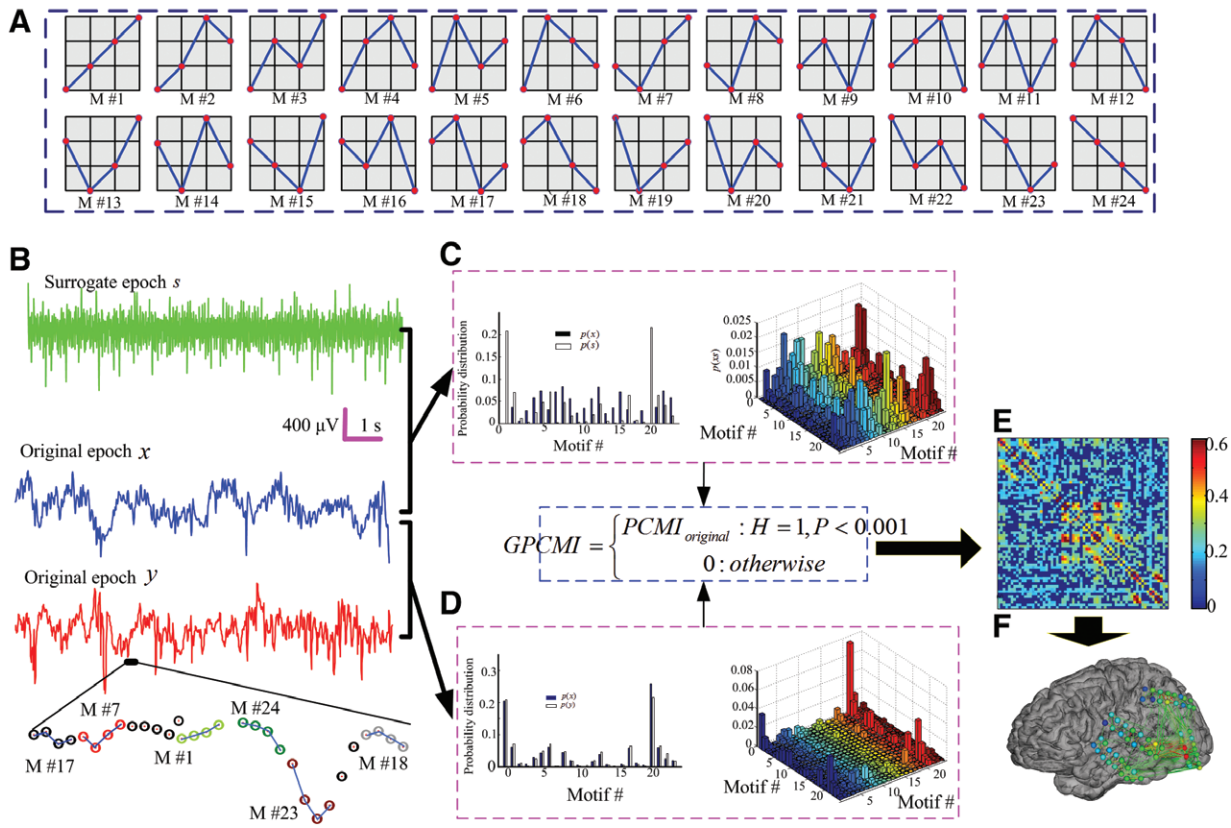

Fig. 1. Diagram of genuine permutation cross mutual information (GPCMI) measurements and GPCMI based cortical networks. (*A*) The motifs (M) of the order 4(4!). (*B*) Two original 10 s electrocorticogram epochs (x and y) from different electrodes, the corresponding surrogate data (s) generated from x and several motifs (order = 4, and lag = 1) from y. (*C*) The probability distributions of x and s, and cross-probability distribution of 10-s times series x and s denoted as p(x), p(s) and p(xs), respectively, with embedding dimension m = 4 and the lag $\tau = 1$. (*D*) The probability distribution and cross-probability distribution of time series x and y, similar to *C*. (*E*) GPCMI matrix between all pairs of channels from one patient at a given time. (*F*) Spatial visualization of the connection matrix in *E*.

$Y_t[y_t, y_{t+\tau}, \ldots, y_{t+m\tau}]$ with embedding dimension m and lag τ, where t is a given sample point.

(2) X_t and Y_t were arranged in ascending order as a symbol of vectors: $[x_{t+(j_1-1)\tau} \le x_{t+(j_2-1)\tau} \le \cdots \le x_{t+(j_m-1)\tau}]$ and $[y_{t+(j_1-1)\tau} \le y_{t+(j_2-1)\tau} \le \cdots \le y_{t+(j_m-1)\tau}]$, respectively.

(3) The marginal probability distribution functions of x_t and y_t were calculated and denoted as $p(x)$ and $p(y)$, respectively. The entropy of x_t and y_t were respectively defined as $H(X) = -\sum_{j=1} p_j \log p_j$ (1)

$$\text{and } H(Y) = -\sum_{j=1}^{J} p_j \log p_j \quad (2)$$

(4) The joint entropy of $H(X,Y)$ was calculated based on the joint probability function.

$$H(X,Y) = -\sum_{x\in X}\sum_{y\in Y} p(x,y)\log p(x,y) \quad (3)$$

(5) The permutation cross mutual information (PCMI) of time series x_t and y_t is:

$$PCMI(X;Y) = H(X) + H(Y) - H(X,Y) \quad (4)$$

(6) Surrogate time series were calculated. To reduce computational complexity, only one time series (*e.g.*, x_t or y_t) was used to generate the surrogate time series. The iterative amplitude-adjusted Fourier transform method was used and the generated surrogate data are denoted x_t^{surr}.[28] We created 50 surrogate time series and calculated their corresponding permutation cross mutual information values, denoted $PCMI_{surr}$.

(7) If the original permutation cross mutual information value, denoted $PCMI_{original}$, deviated significantly from the distribution of the $PCMI_{surr}$, the $PCMI_{original}$ was considered to be a genuine permutation cross mutual information, or a true connection. Otherwise, the $PCMI_{original}$ was considered a spurious permutation cross mutual information (denoted $PCMI_{spur}$).

The Wilcoxon signed-rank test (*signrank.m* in MATLAB) was used in the above significance testing. The median of $PCMI_{surr}$ was tested with the $PCMI_{original}$. If $H_0 = 1$ and $p < 0.001$, $GPCMI = PCMI_{original}$. Otherwise, $GPCMI = 0$, which was called $PCMI_{spur}$. In this study, the genuine permutation cross mutual information (GPCMI) calculation can be described as:

$$GPCMI = \begin{cases} PCMI_{original} : H = 1, P < 0.001 \\ 0 : otherwise \end{cases} \quad (5)$$

The choice of embedding dimension m, lag τ, and *epoch length* is crucial to the permutation cross mutual information calculation. If the embedding dimension is too small ($m = 1$ or 2), the scheme will not work, because there will not be enough distinct states in the time series. On the other hand, the epoch length of the time series should be larger than $m! \times m!$ to achieve a proper differentiation between stochastic and deterministic dynamics. Parameter selection is discussed in Supplemental Digital Content 2 (part 1, http://links.lww.com/ALN/C71). Based on the model and testing on real electroencephalogram data, $m = 4$, $\tau = 1$, and epoch length of 10 s with an overlap of 75% were chosen for permutation cross mutual information calculation.

Thus, there are three permutation cross mutual information–based indices in this study: (1) The original permutation cross mutual information is the value derived from the permutation cross mutual information algorithm. (2) The surrogate permutation cross mutual information is the permutation cross mutual information value derived from surrogate data. (3) The genuine permutation cross mutual information is the permutation cross mutual information value after the Wilcoxon signed-rank test. The genuine permutation cross mutual information could be zero (not significantly deviating from the distribution of the $PCMI_{surr}$ indices, which were derived from the surrogate data), or equal to the original permutation cross mutual information value (significantly deviating from the distribution of the $PCMI_{surr}$ indices). Thus, the genuine permutation cross mutual information values were divided into two groups: nonzero and zero.

In calculating genuine connectivity, Lee *et al.*[27] used the original connection index minus the median of the surrogate connectivity indices to define the genuine connectivity under $H_0 = 1$ and $P < 0.05$. Because the signals of nearby but separate channels are naturally correlated, we selected $P < 0.001$ as the threshold for the genuine permutation cross mutual information calculation. Because permutation cross mutual information values were low when using $m = 4$ and $\tau = 1$, the median of $PCMI_{surr}$ may exceeded $PCMI_{original}$ in some cases. Thus, the $PCMI_{original}$ minus the median of the $PCMI_{surr}$ would have given a meaningless value in these situations. Therefore, we termed the genuine permutation cross mutual information as $PCMI_{original}$ when $H_0 = 1$ and $P < 0.001$.

Genuine Cortical Networks

This study used graph theory to explore variations in the mesoscale brain networks of different anesthesia states. We termed this brain network at a cortical scale the *cortical network*. Each node in the graph corresponded to an electrode, and the genuine permutation cross mutual information values between electrodes' electrocorticogram time series acted as edge weights. For each patient, we defined the cortical network as consisting of all nodes and the corresponding edge weights mapped from the genuine permutation cross mutual information matrix. In this study, we only considered undirected functional connections; weighted graphs were used to analyze the cortical network to avoid choosing an arbitrary threshold for binary graph analysis.

Metrics from graph theory can be used to characterize a brain network at both nodal (specific nodes or regions within the network) and global levels.[29] Regional and nodal characteristics of the cortical network were measured by the nodal clustering coefficient and the nodal efficiency. The average clustering coefficient and metrics of average path length were used as global network measures. These measures have been used to describe functional brain networks in both healthy and diseased subjects,[30,31] as well as in propofol-induced unconsciousness at the macro scale.[27]

The clustering coefficient of one node is the number of its neighboring nodes that are connected to each other divided by its total nodal connections. This study used a modified version of the clustering coefficient introduced by Stam *et al.*[32] The nodal clustering coefficient of node i is defined as

$$NCC_i = \frac{\sum_{j \neq i} \sum_{m \neq i, m \neq j} w_{ij} w_{im} w_{jm}}{\sum_{j \neq i} \sum_{m \neq i, m \neq j} w_{ij} w_{im}} \quad (6)$$

where w is the edge weight (estimated using the genuine permutation cross mutual information in this study) between two nodes. The average clustering coefficient (C_{ave}) of the whole cortical network (global level) is defined as

$$C_{ave} = \frac{1}{N} \sum_{i=1}^{N} NCC_i \quad (7)$$

where N is the total number of nodes. A large clustering coefficient indicates that a node is highly interconnected with its neighbors, so a high average clustering coefficient means a network is highly interconnected.

Nodal efficiency characterizes the efficiency of a node at exchanging messages with the other nodes of the network (nodal level). The efficiency of node (E_{nod}) i is defined as[33]

$$E_{nod}(i) = \frac{1}{N-1} \sum_{j \neq i \in G} \frac{1}{d_{ij}} \quad (8)$$

where d_{ij} is the shortest path length between node i and j.[34] The shortest path is defined as the path with the shortest length between the two nodes in the graph. The length of an edge between node i and j is the inverse of the

weight w_{ij} (*i.e.*, $L_{ij} = 1/w_{ij}$). The d_{ij} can be calculated based on the weight network.[35]

The average path length is the average of the shortest path lengths (d_{ij}) between all pairs of channels in the cortical network. This reflects the global efficiency of information transmission in a network, so a shorter path length indicates faster information transmission in the brain. A harmonic mean was used to prevent the appearance of an infinite average path length (L_{ave}) due to disconnected links.[34]

$$L_{ave} = \frac{1}{\frac{1}{N(N-1)}\sum_{i=1}^{N}\sum_{j\neq i}^{N}(1/d_{ij})} \quad (9)$$

Because of the irregular distribution of the electrocorticogram recording strips on the surface of cortical regions, the cortical networks in this study only reflect the characteristics of the area covered by the strips, not the whole brain. However, the variation in distance between the electrodes did not influence the network parameters.

We normalized the observed clustering coefficient and path length by using corresponding metrics calculated from random networks. The random networks were generated from the original networks. The random networks preserved the degree distribution while edges were shuffled.[36] We denote the average clustering coefficient and path length of a random network as C_r and L_r, respectively. To calculate the normalized C_{ave} and L_{ave}, the C_{ave} and L_{ave} were divided by the C_r and L_r, and denoted as C_{ave}/C_r (*i.e.*, normalized average clustering coefficient) and L_{ave}/L_r (*i.e.*, normalized average path length), respectively. Also, the small worldness index (σ) was calculated as the ratio of C_{ave}/C_r to L_{ave}/L_r.

Similar to the calculation of permutation cross mutual information, all of the cortical network parameters were calculated for each 10 s of electrocorticogram data, so as to estimate the time evolution of network changes. To compare wakeful and unconscious states, the cortical networks' indices for all windows in each state were averaged.

Electrode Distance Quantification and Cortical Region Classification

Because the electrocorticogram recording strips were irregularly distributed on the cortical surface and there were no magnetic resonance imaging data for the patients, we were unable to specify the exact underlying anatomical structures and coordinates for the electrodes. To determine the electrodes' distances, several procedures were used, as described below:

Based on clinical records and electrode photographs of every patient, we projected all electrodes to a standard brain model, based on the Brain Function Mapping toolbox developed by our team.[37] Thus we established the coordinate values for all electrodes in a standard brain model space. The electrodes on each strip were fixed in location, so we termed this distance the *linear strip distance*. It incorporates the curvature of the brain's surface. Based on the coordinate values of all electrodes, we used the following procedure to group pairs of electrodes with similar linear surface distance into seven distance groups. Consider 1 cm as an example. First, all 1-cm strip distance electrodes pairs from a single strip were included. Then, all linear Euclidean distances between pairs of electrodes—whose strip distance was 1 cm—were calculated based on their coordinate values. Next, we calculated the mean and SD of these distances and termed the distance the *space distance* of 1 cm. Finally, we calculated all distances between pairs of electrodes from different strips based on their coordinate values, and included electrode pairs whose distance met the criterion of a space distance of 1 cm. When two rows were present on one strip, we adopted a rounding approach to classify them. For example, electrodes with strip distance of 1.414 cm were enrolled in the group of 1 cm. Electrodes pairs with a surface distance of more than 7 cm were classified as 7 cm for statistics. Based on this grouping procedure, the numbers of pairs for each distance group were 805 (1 cm), 943 (2 cm), 1,204 (3 cm), 1,381 (4 cm), 1,422 (5 cm), 1,544 (6 cm), and 1,610 (7 cm).

This study uses two different brain region classification methods. The first is to roughly divide the brain into four regions: frontal, parietal, temporal, and occipital. For all eight patients, the number of electrodes in the frontal, parietal, temporal, and occipital regions were 120, 211, 104, and 61, respectively. The second is based on the standard Brodmann areas. We used Brain Voyager Brain Tutor to remap all electrodes to Brodmann's areas. All electrodes for the eight patients are shown in figure 2. The numbers of electrodes in each Brodmann area are listed in Supplemental Digital Content 3 (http://links.lww.com/ALN/C72).

Eliminating Volume Conduction Effects Based on Independent Component Analysis

Unlike scalp electroencephalogram, the electrocorticogram records neural activity directly from the cortical surface. Thus, the spatial spread of brain source currents passing through the dura, scalp, and skull only exerts minor influence over it. Therefore, most electrocorticogram studies have ignored volume conduction effects when measuring cortical networks.[38–40] However, other researchers have suggested that volume conduction effects should be considered in electrocorticogram signal analysis. Compared with scalp electroencephalogram and magnetoencephalography recordings, source-reconstruction of electrocorticogram signals is underdeveloped.[41] Fischer *et al.*[42] used envelope intrinsic coupling modes, which are not affected by zero-phase lagged components, to eliminate the volume conduction effects. Other studies[25,26] used independent component analysis as a spatial-temporal filter to solve the volume conduction problem in electrocorticogram signals. Hindriks *et al.*[41] proposed using source-space spatial independent component analysis to identify the generators of cortical rhythms and to reconstruct functional connectivity.

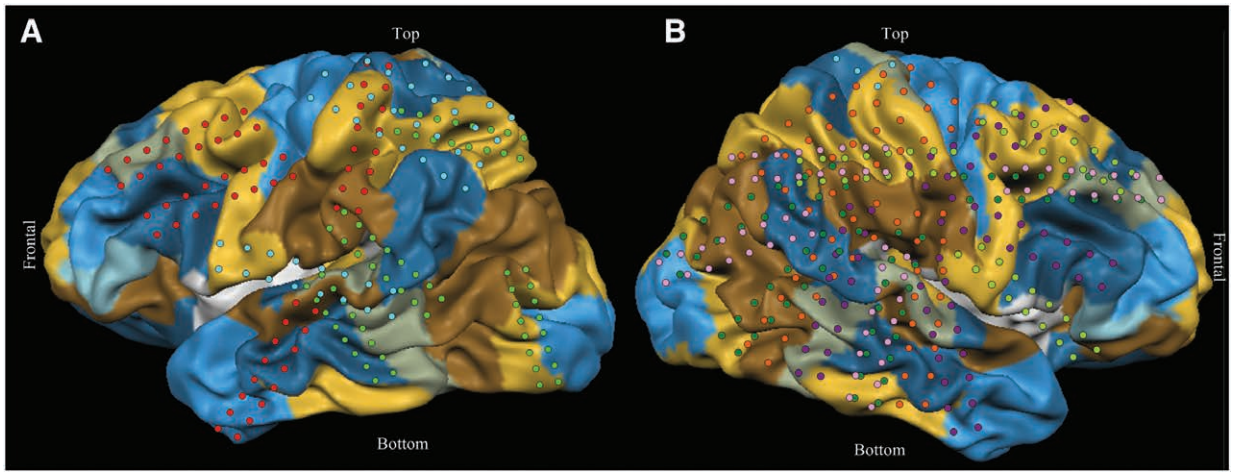

Fig. 2. Electrode locations for all patients on a standard brain model. *A* and *B* are views from the left and right hemispheres, respectively.

Another study[25] used a sum of four independent components to replace the original signal. The investigators found that the waveform similarity among independent components was lower compared with the original electrode signals, as assessed by the distribution of pair-wise squared Pearson correlation values between independent components *versus* between electrodes.

Therefore, we employed a similar method to attenuate the influence of volume conduction effects. The procedure is as follows:

(1) The raw 64-channel electrocorticogram signals were decomposed, using the fast independent component analysis algorithm.
(2) We calculated the weights of the independent components for each channel based on the percent variance accounted for method.[25]
(3) We searched the channel pairs to find those which had three common sources (independent components) in their first five largest independent components; we inferred that these came from the same sources.
(4) The common source channels were replaced by their first five largest independent components, excluding the common source for permutation cross mutual information calculation. The paired channels that did not have a common source were calculated using the original signal.

Details of the analysis are shown in Supplement Digital Content 2 (part 3, http://links.lww.com/ALN/C71).

The Influence of Studying an Epileptic Brain

Various studies of patients with refractory epilepsy during anesthesia have found epileptiform spiking in the electrocorticogram.[43–45] In this study, we analyzed spiking influence on the permutation cross mutual information, detailed in Supplemental Digital Content 2 (part 2, http://links.lww.com/ALN/C71). The results show that permutation cross mutual information indices can robustly track the coupling strength of the simulated model, even when there is a significant amount of spiking. There was only about a 2% to 3% offset from the original permutation cross mutual information when there was a high spike rate of one spike per second.

Statistical Analysis

The samples in this study were selected in accordance with previous experiments and to reduce patient burden. No *a priori* statistical power calculation was conducted to guide sample size.

R Project (version 3.5.3; http://www.r-project.org; accessed March 20, 2019) and MATLAB Toolbox were used for statistical analysis. The statistical analysis included the following steps: The Liliefors test (*lilietest.m*) was used to determine whether indices were normally distributed. Then, we analyzed the nonzero genuine permutation cross mutual information value changes from wakefulness (the state before drug induction) to early unconscious states (the time span from loss of consciousness to 200 s after loss of consciousness), and late unconscious state (the time span from 200 s after loss of consciousness to end of recordings) in different electrodes and different cortical regions. A generalized linear mixed model with Satterthwaite's method was applied to analyze the interaction effects of the three factors: (1) state (three levels: wakefulness, early unconscious state, and late unconscious state), (2) distance (seven levels: linear surface distance from 1 cm to 7 cm with 1-cm steps), and (3) region (six levels: frontal-frontal, parietal-parietal, temporal-temporal, frontal-parietal, frontal-temporal, parietal-temporal). Generalized linear mixed model analysis allows more flexibility with missing

values and can deal with individual differences by using a random intercept for individual participants. In this study, the fixed effects were state, distance, and region; the random effects were the random intercept for each subject. After obtaining the interaction effects of the three factors, the mean and 95% CI values of the estimated difference (two-sides) are reported. A Tukey test was used for *post hoc* testing. Adjusted P values of less than 0.05 were considered to be significant. In the figures, $P < 0.05$, $P < 0.01$, $P < 0.001$ are marked with the notations of "★", "★★", and "★★★", respectively. Cohen's d was used to calculate the effect size for the mixed effects model.[46]

Given the inconsistency of electrode coverage between subjects, we set the following enrollment criteria for statistics: (1) more than 20 electrodes in the region, (2) more than four patients with electrodes in the region. The nodal network parameters nodal clustering coefficient and nodal efficiency used a similar statistical test for significance. One-way ANOVA was used to analyze the significance between the three states for the global network parameters of C_{ave}/C_r, L_{ave}/L_r, and σ.

Results

Description of the Schematic Diagram of Genuine Permutation Cross Mutual Information and Electrocorticogram Recording Analysis

In this study, we set the embedding dimension $m = 4$ and lag $\tau = 1$ for the permutation cross mutual information calculation. The ordinal patterns for $m = 4$ are depicted in figure 1A. There are $4! = 24$ motifs. Figure 1B displays 10-s electrocorticogram epochs from two electrodes (x and y) and associated surrogate data for x. Some of the motifs in the original electrocorticogram epoch y are shown in the lower section. Surrogate permutation cross mutual information values can be calculated based on the surrogate epoch s, and examples of the probability distribution and cross-probability distribution are shown in figure 1C. The original electrocorticogram epochs of x and y produced the original permutation cross mutual information values, as well as the probability distribution and cross-probability distribution shown in figure 1D. The embedded dimension $m = 4$ and lag $\tau = 1$ parameters were selected based on our previous study.[47] Based on the calculations of original and surrogate permutation cross mutual information, the genuine permutation cross mutual information values can be achieved. Figure 1E showed the genuine permutation cross mutual information matrix values derived from the 64 channels electrocorticogram recordings. The associated spatially visualized connections are shown in figure 1F.

Figure 3 shows a typical example of cortical network calculation based on the genuine permutation cross mutual information. Figure 3A shows a photograph of the intraoperative intracranial electrocorticogram monitoring (*upper*) and the spatial distribution of the 64 electrodes (*lower*) for one patient. Four electrode strips were implanted in left and posterior temporal (8 × 2, channel 1–16), left parietal and occipital lobes (8 × 2, channel 17–32), left bottom occipital and occipital pole (8 × 2, channel 33–48), and left occipital and interhemispheric (8 × 2, channel 49–64). The electrodes mainly covered the Brodmann areas of 5, 7, 17, 18, 19, 21, 22, 37, 39, 40, 41, and 42. Detailed functions of these cortical regions are presented in Supplemental Digital Content 3 (http://links.lww.com/ALN/C72). Figure 3B shows the raw electrocorticogram signals acquired during anesthesia induction, with two enlarged 5-s segments for exemplary electrodes.

We examined the changes in cortical networks during the induction process of anesthesia in one patient as a case study. We selected five time points from the whole anesthesia procedure: wakefulness, time points of 30 s, 90 s, 150 s, and 210 s after loss of consciousness. The genuine permutation cross mutual information matrices at these five time points are presented in figure 3C. Electrode coverage included temporal (n = 16), parietal (n = 8), and occipital (n = 40) cortical areas for this patient. It can be observed that genuine permutation cross mutual information values decreased after loss of consciousness, and genuine permutation cross mutual information values in the occipital area were higher than those in the parietal region. The corresponding spatial connections are shown in figure 3D. The nodal clustering coefficient and nodal efficiency of the cortical network for the whole procedure are presented in figure 3E and 3F. Nodal clustering coefficient progressively decreased while nodal efficiency decreased abruptly around the point of loss of consciousness.

Information Integration over Local and Distant Cortical Regions

To analyze the time course of information integration changes from the awake state to unconsciousness in terms of local *versus* distant connectivity, four electrocorticogram recordings with differing linear surface distances were selected. As seen in figure 4, we analyzed the same patient shown in figure 3. This patient had four electrode strips (fig. 4A) and figure 4B shows the arrangement diagram and distance labels of electrode strip 1. Electrode pairs 1 and 2 or 1 and 9, or 2 and 9 (1 cm to 1.414 cm distance) were regarded as local; whereas electrode pairs 1 and 8, 2 and 8, and 8 and 9 (6 cm to 7 cm distance) were regarded as distant. The electrocorticogram recordings of channels 1, 2, 8, and 9 were showed in figure 4C.

Figure 4D reveals an interesting phenomenon. The nonzero genuine permutation cross mutual information values of the local raw electrocorticogram recordings increased after loss of consciousness. Studies have found that signals recorded from close electrodes might appear similar as a result of the volume conduction effect.[25,26,48] After the independent component analysis–based procedure to reduce volume conduction effects, the genuine permutation cross mutual information values of short distances decreased after loss of

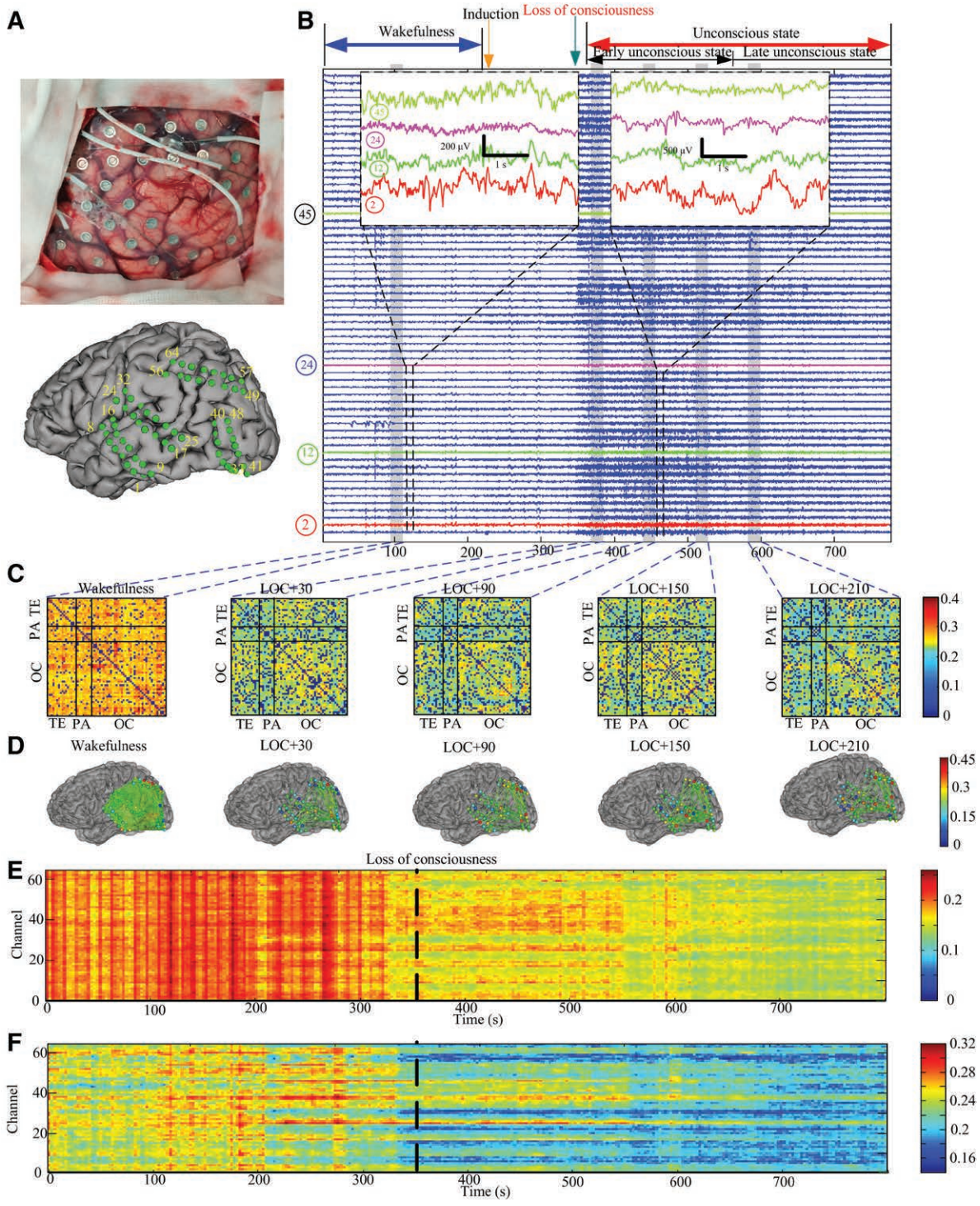

Fig. 3. Example of the changes in the genuine permutation cross mutual information (GPCMI)–based network topology for one patient transitioning from wakefulness to unconsciousness. (*A*) Intraoperative electrocorticogram monitoring photograph and spatial topography of the 64 electrodes of one patient. (*B*) Raw electrocorticogram recordings of all channels during the whole time course from wakefulness to unconscious state and two enlarged 5-s segments of channels 2, 12, 24, and 45 in wakefulness (phase before anesthesia induction) and unconscious states (phase after loss of consciousness [LOC]). (*C*) GPCMI among all nodes at wakefulness, LOC + 30, LOC + 90, LOC + 150 and LOC + 210. Temporal (TE; n = 16), parietal (PA; n = 8), and occipital (OC; n = 40). (*D*) The spatial distributions of GPCMI shown in *C*. (*E* and *F*) The time course of nodal clustering coefficients and nodal efficiency, respectively, for each electrode. LOC + 30, LOC + 90, LOC + 150, and LOC + 210 represent the time points of 30 s, 90 s, 150 s, and 210 s after loss of consciousness, respectively.

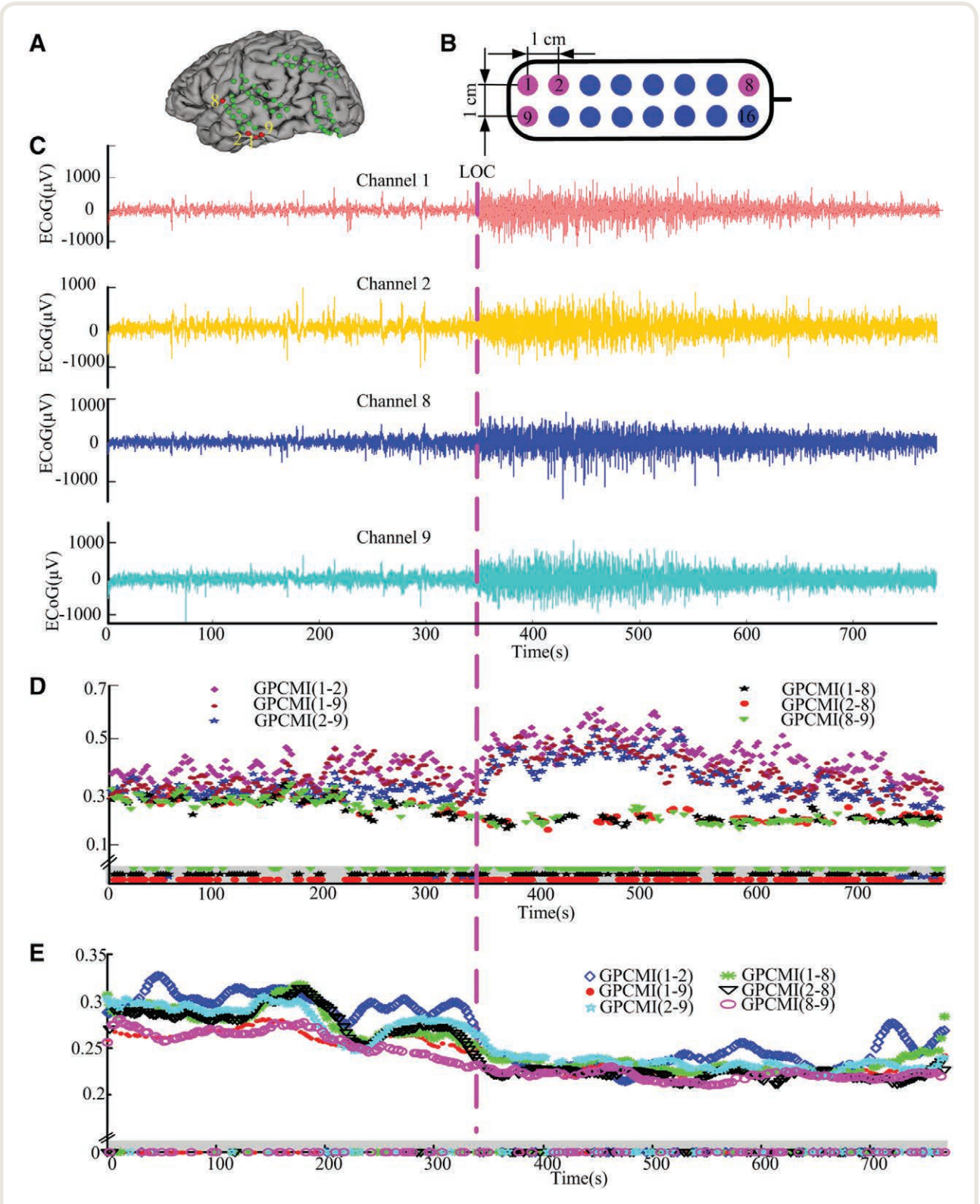

Fig. 4. Electrocorticogram recordings of four channels from one patient and corresponding electrocorticogram measures *versus* time. (*A*) Spatial topography of the 64 electrodes of one patient. (*B*) Arrangement diagram of electrode strip 1 and distance labeling. (*C*) Raw electrocorticogram recordings for channels 1, 2, 8, and 9 of the patient. (*D*) Time course of genuine permutation cross mutual information (GPCMI) values for raw electrocorticogram signals. (*E*) Time course of GPCMI values for independent component analysis based signals. LOC, loss of consciousness.

consciousness (fig. 4E). This means that volume conduction may be an important factor in an observed, but perhaps spurious, local increase in permutation cross mutual information.

Also, the nonzero genuine permutation cross mutual information curves of raw electrocorticogram signals correlate with electrocorticogram amplitude. Thus, we reanalyzed the power of these channels. The results are shown in Supplemental Digital Content 2 (part 4, http://links.lww.com/ALN/C71). The relative power spectrum density was used to analyze the power for each frequency band. Figure S26C through S26F (Supplemental Digital Content 2, part 4, http://links.lww.com/ALN/C71) shows that the relative power spectrum density in the delta increased after loss of consciousness. However, the relative power spectrum density values in the waking state were not consistent across the four channels. Therefore, we cannot say that the amplitude reliably tracks the effect concentration of the propofol. The permutation cross mutual information is calculated *via* symbolic dynamics and mutual information. The central procedure of symbolic dynamic analysis is discretizing the time-series into a corresponding sequence of symbols by comparing neighboring time points.[9] Therefore, the permutation cross mutual information is more closely related to the relative amplitude than to the absolute amplitude of the signal. Combined with the results of the independent component analysis–based analysis, we concluded that the observed local increase in permutation cross mutual information was mainly due to the influence of volume conduction, not the amplitude of electrocorticogram.

In this study, we found clear beta activity approximately 150 s before loss of consciousness for this patient (see fig. S25 in Supplemental Digital Content 2, part 4, http://links.lww.com/ALN/C71). A previous electroencephalogram study[49] reported that beta power increased in the frontal/central area in light sedation by propofol. In deep sedation, alpha oscillations dominated the frontal area. With loss of consciousness, slow wave oscillations (delta and theta power) increased in the frontal area. However, not all patients had obvious beta oscillations before loss of consciousness. As shown in figure S27 in Supplemental Digital Content 2 (part 4, http://links.lww.com/ALN/C71), there was no consistent sustained beta wave phenomenon before the loss of consciousness time point. Because anesthesia induction is not a stable state but a dynamic process, the nonzero genuine permutation cross mutual information had an abrupt change during this process. It is not appropriate to treat this process as a state for analyzing. Therefore, we did not analyze the electrocorticogram recordings of the time span between the drug delivery time and loss of consciousness time.

Nonzero Genuine Permutation Cross Mutual Information Indices Change with Distance under Different Anesthesia Conditions

The nonzero genuine permutation cross mutual information index represents the connection strength between two nodes. The nonzero genuine permutation cross mutual information for wakeful and unconscious states (early and late), and for electrode distance from 1 to 7 cm, is summarized in figure 5A. Because electrode pairs may belong to different distances classes and different cortical regions, we used generalized linear mixed-model regression to analyze the interactions of the factors of state (waking, early, and late unconsciousness), distances (from 1 cm to 7 cm), and brain regions (frontal, parietal, and temporal). ANOVA showed that there was no three-way interaction effect between the factors of state, distance, and region, $F(36, 9832.1) = 0.97$, $P = 0.512$. Given that the three-way interaction effect was not significant, we tested whether the three two-way interaction effects were significant. The results showed that the interaction effects between state and region, and between region and distance were statistically significant, $F(6, 9833.1) = 14.65$, $P < 0.001$, and $F(18, 9833.3) = 14.22$, $P < 0.001$, respectively). The interaction effect between state and distance was not significant, $F(12, 9832.2) = 0.76$, $P = 0.687$.

This study focused on information integration changes at different electrode distances and different cortical regions during propofol anesthesia. It can be seen that the distribution of nonzero genuine permutation cross mutual information values decreases with increasing separation distance, in both waking and unconscious states (early and late; fig. 5A), especially for distances less than 3 cm. The median and first quartile, third quartile of the indices were calculated and are presented in table 1. Because there was no interaction between state and distance, we analyzed the nonzero genuine permutation cross mutual information with different distances in different cortical regions. Based on the enrollment criteria, only nonzero genuine permutation cross mutual information indices in the frontal, parietal, temporal, and parietal-temporal regions were considered in this study. The significant tests for *post hoc* comparison and the contrasts of difference with a 95% CI between the indices in all distances are shown in Supplemental Digital Content 4 (http://links.lww.com/ALN/C73). It can be seen that there were no significant differences in any of the cortical regions (frontal, parietal, temporal, or parietal-temporal) at a distance more than 3 cm (all P values are more than 0.05 [Tukey test]). This suggests that information integration decreases with increased separation between two brain regions, both in waking and unconscious states. Also, the effect size values of those with P values less than 0.05 were calculated. It can be seen that effect size values between the distance of 1 cm and 3 cm to 7 cm in temporal and parietal regions are high (greater than 1 cm). This means that the overlap between the nonzero genuine permutation cross mutual information values at 1 cm and at other distances (3 cm to 7 cm) are tiny and that the effects are significant.

The percentage of genuine connections is an index on the efficiency of communication. Overall, the percentage of genuine connections in the wakeful state was more than in early unconscious and late unconscious states (fig. 5B and table 2). generalized linear mixed model analysis for

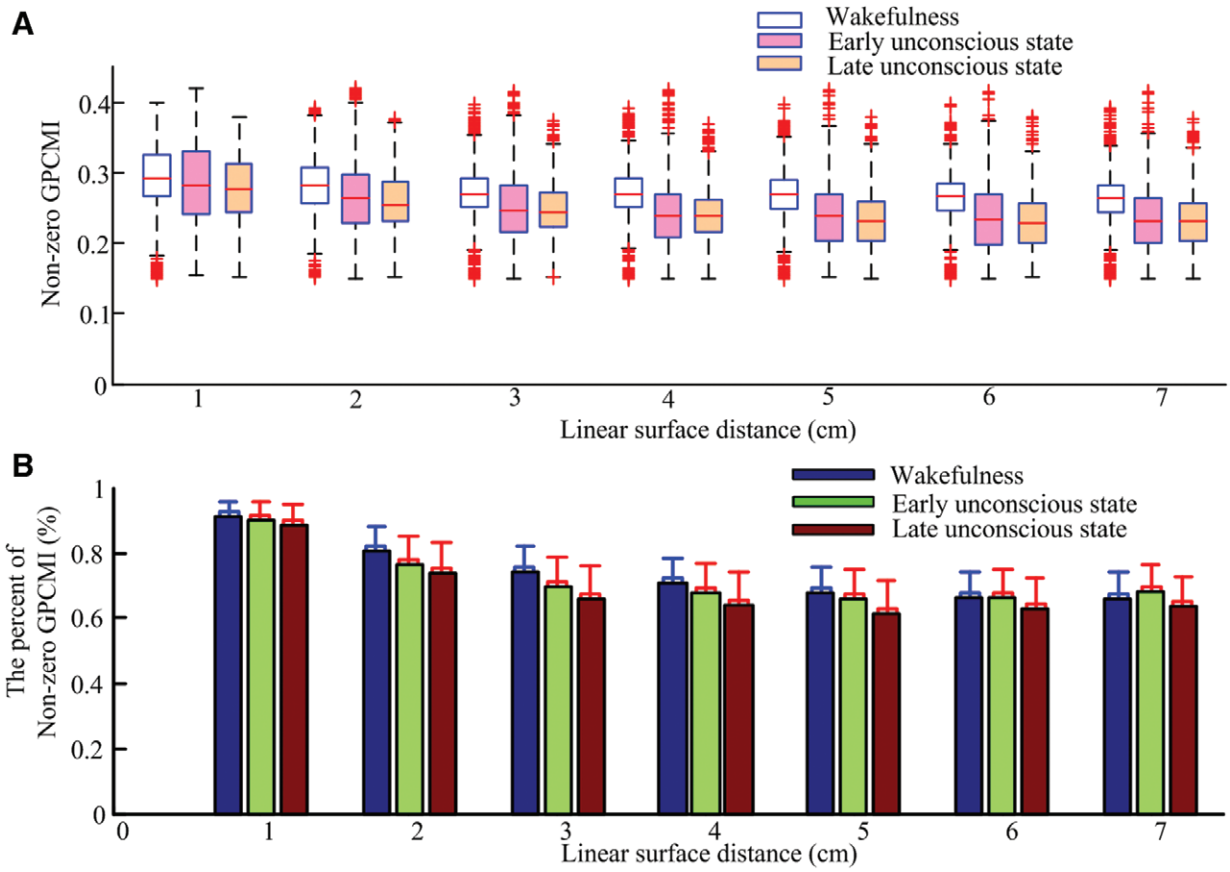

Fig. 5. Statistics for genuine permutation cross mutual information (GPCMI) indices from wakefulness, early unconscious state, and late unconscious state. (*A*) Box plots of nonzero GPCMI at distance from 1 cm to 7 cm. Lower and upper lines of the box are the 25th and 75th percentiles of the sample, respectively, the middle red line of the box is the median, and the distance between the top and bottom of the box is the interquartile range. Outliers (*red +*) are indices that are more than 1.5 times the interquartile range away from the median. (*B*) Nonzero GPCMI percentage at different distances for all patients in wakefulness, early unconscious state, and late unconscious state.

percentage of genuine connections showed that the factors of state, region, and distance had three-way interaction effects, $F(36, 11136) = 1.46$, $P = 0.027$). The interaction effects between state and region, region and distance, as well as state and distance, were statistically significant, $F(6, 11136) = 13.23$, $P < 0.001$; $F(18,11137) = 8.38$, $P < 0.001$; and $F(12,11136) = 2.36$, $P = 0.005$, respectively. Multiple comparison and significance test results, effect size, as well as the contrasts of difference with a 95% CI among different distances in wakeful and unconscious states (early and late) are shown in Supplemental Digital Content 5 (http://links.lww.com/ALN/C74). It is noteworthy that the nonzero genuine

Table 1. The Median and First Quartile, Third Quartile of Nonzero Genuine Permutation Cross Mutual Information Values with the Distance Range from 1 to 7 cm in the Wakefulness, Early Unconscious State, and Late Unconscious State

Distance (cm)	Wakefulness Median (1st, 3rd quartile)	Early Unconscious State Median (1st, 3rd quartile)	Late Unconscious State Median (1st, 3rd quartile)
1	0.29 (0.27, 0.33)	0.28 (0.24, 0.33)	0.28 (0.25, 0.31)
2	0.28 (0.26, 0.31)	0.27 (0.23, 0.30)	0.26 (0.23, 0.29)
3	0.27 (0.25, 0.29)	0.25 (0.22, 0.28)	0.24 (0.22, 0.27)
4	0.27 (0.25, 0.29)	0.24 (0.21, 0.27)	0.24 (0.22, 0.26)
5	0.27 (0.25, 0.29)	0.24 (0.20, 0.27)	0.23 (0.20, 0.26)
6	0.27 (0.25, 0.29)	0.24 (0.20, 0.27)	0.23 (0.20, 0.26)
7	0.27 (0.24, 0.28)	0.23 (0.20, 0.26)	0.23 (0.20, 0.26)

Table 2. The Percent Values of the Nonzero Genuine Permutation Cross Mutual Information Number in All Genuine Permutation Cross Mutual Information of Different Distance in Wakefulness, Early Unconscious State, and Late Unconscious State

Distance (cm)	Wakefulness Mean ± SD	Early Unconscious State Mean ± SD	Late Unconscious State Mean ± SD
1	0.91 ± 0.04	0.90 ± 0.05	0.88 ± 0.06
2	0.80 ± 0.07	0.76 ± 0.08	0.73 ± 0.09
3	0.74 ± 0.07	0.69 ± 0.09	0.65 ± 0.09
4	0.70 ± 0.07	0.67 ± 0.09	0.64 ± 0.09
5	0.67 ± 0.08	0.65 ± 0.09	0.61 ± 0.10
6	0.66 ± 0.07	0.66 ± 0.08	0.62 ± 0.09
7	0.65 ± 0.08	0.68 ± 0.08	0.63 ± 0.09

permutation cross mutual information percentages for linear surface distances less than 2 cm were significantly higher than those from greater distances, in both wakefulness and unconscious states in all cortical regions (all P values are less than 0.05 [Tukey test]). For each distance, there were no significant differences between the states of wakefulness and early and late unconscious states (all P values are more than 0.05 [Tukey test]). In temporal and parietal regions, the effect size values between the distances of 1 cm and 3 cm to 7 cm were above 0.5 (medium effect size).

Information Integration in Intra- and Inter-regional Connections during Propofol Anesthesia

We further analyzed information integration between and within different brain areas. We considered two different cortical division methods. The first one was based on rough anatomical division. Our electrodes only covered the temporal, parietal, occipital, and frontal regions. Based on our statistical criteria (1: more than 20 electrodes in this region, 2: more than 4 patients have electrodes in this region), only temporal, parietal, and frontal were selected for intra-regional connection analysis. Also, only the parietal-temporal connection was selected for inter-region analysis. The above intra- and inter-regional connections are shown in figure 6A and 6B, respectively. For the intra-region nonzero genuine permutation cross mutual information (electrode pairs for nonzero genuine permutation cross mutual information calculation came from the same cortical region), pairs distances less than 6 cm were included. Conversely, for inter-region nonzero genuine permutation cross mutual information (electrode pairs came from two different cortical regions), we only considered pair distances greater than 3 cm. For the inter-regional connection between Brodmann areas, as shown in figure 6C, only the nonzero genuine permutation cross mutual information of the Brodmann area 7 *versus* Brodmann area 20, Brodmann area 39 *versus* Brodmann area 20, Brodmann area 39 *versus* Brodmann area 41, BA40 *versus* Brodmann area 20, and Brodmann area 40 *versus* Brodmann area 41 were considered for statistical analysis.

The results of the generalized linear mixed model analysis on nonzero genuine permutation cross mutual information showed that there were interaction effects between cortical region and state. This means that the changes in intra-regional integration of information during propofol-induced anesthesia were related to both cortical region and anesthesia state. *Post hoc* comparison showed that the awake state nonzero genuine permutation cross mutual information was significantly higher than early unconscious state nonzero genuine permutation cross mutual information (frontal: 0.018 [0.009, 0.026], $P < 0.001$, $d = 0.26$; parietal: 0.038 [0.031, 0.043], $P < 0.001$, $d = 0.54$; temporal: 0.009 [0.002, 0.016], $P = 0.018$, $d = 0.13$; temporal-parietal: 0.042 [0.031, 0.055], $P < 0.001$, $d = 0.62$. The generalized linear mixed model analysis showed that the factors of Brodmann area and state have interaction effects, $F(8,3336.8) = 3.06$, $P = 0.006$). *Post hoc* comparison of different anesthesia states in each Brodmann area showed that the wakeful state is significantly higher than early unconscious state (Brodmann areas 7–20: 0.048 [0.040, 0.056], $P < 0.001$, $d = 0.201$; Brodmann areas 39–20: 0.049 [0.037, 0.062], $P < 0.001$, $d = 0.205$; Brodmann areas 39–41: 0.028 [0.009, 0.046], $P < 0.001$, $d = 0.115$; Brodmann areas 40–20: 0.053 [0.042, 0.064], $P < 0.001$, $d = 0.221$; Brodmann areas 40–41: 0.022 [0.006, 0.038], $P < 0.001$, $d = 0.093$), as well as late unconscious state (Brodmann areas 7–20: 0.041 [0.030, 0.052], $P < 0.001$, $d = 0.168$; Brodmann areas 39–20: 0.046 [0.034, 0.059], $P < 0.001$, $d = 0.192$; Brodmann areas 39–41: 0.028 [0.009, 0.046], $P < 0.001$, $d = 0.116$; Brodmann areas 40–20: 0.048 [0.038, 0.059], $P < 0.001$, $d = 0.199$; Brodmann areas 40–41: 0.020 [0.005, 0.037], $P < 0.001$, $d = 0.086$), whereas there were no significant differences between early and late unconscious states in any of the Brodmann area (all P values are more than 0.05, Tukey test). The median (first quartile, third quartile) nonzero genuine permutation cross mutual information indices for intra- and inter-regional connections are presented in table 3.

Cortical Network Changes at Nodal and Global Levels during Propofol-induced Unconsciousness

At the nodal level, we analyzed the nodal clustering coefficients and nodal efficiency. Figure 7A and 7B show the nodal clustering coefficients and nodal efficiency values of seven Brodmann areas in waking, early unconscious state, and late unconsciousness state. Based on our selection criteria, the Brodmann areas of primary motor cortex (Brodmann area 4), premotor cortex and supplementary motor cortex (Brodmann area 6), visuo-motor coordination (Brodmann area 7), temporal gyrus (Brodmann areas 20, 21, 22), angular gyrus (Brodmann area 39), supramarginal gyrus (Brodmann area 40), and auditory cortex (Brodmann areas 41, 42) were enrolled for statistical analysis.

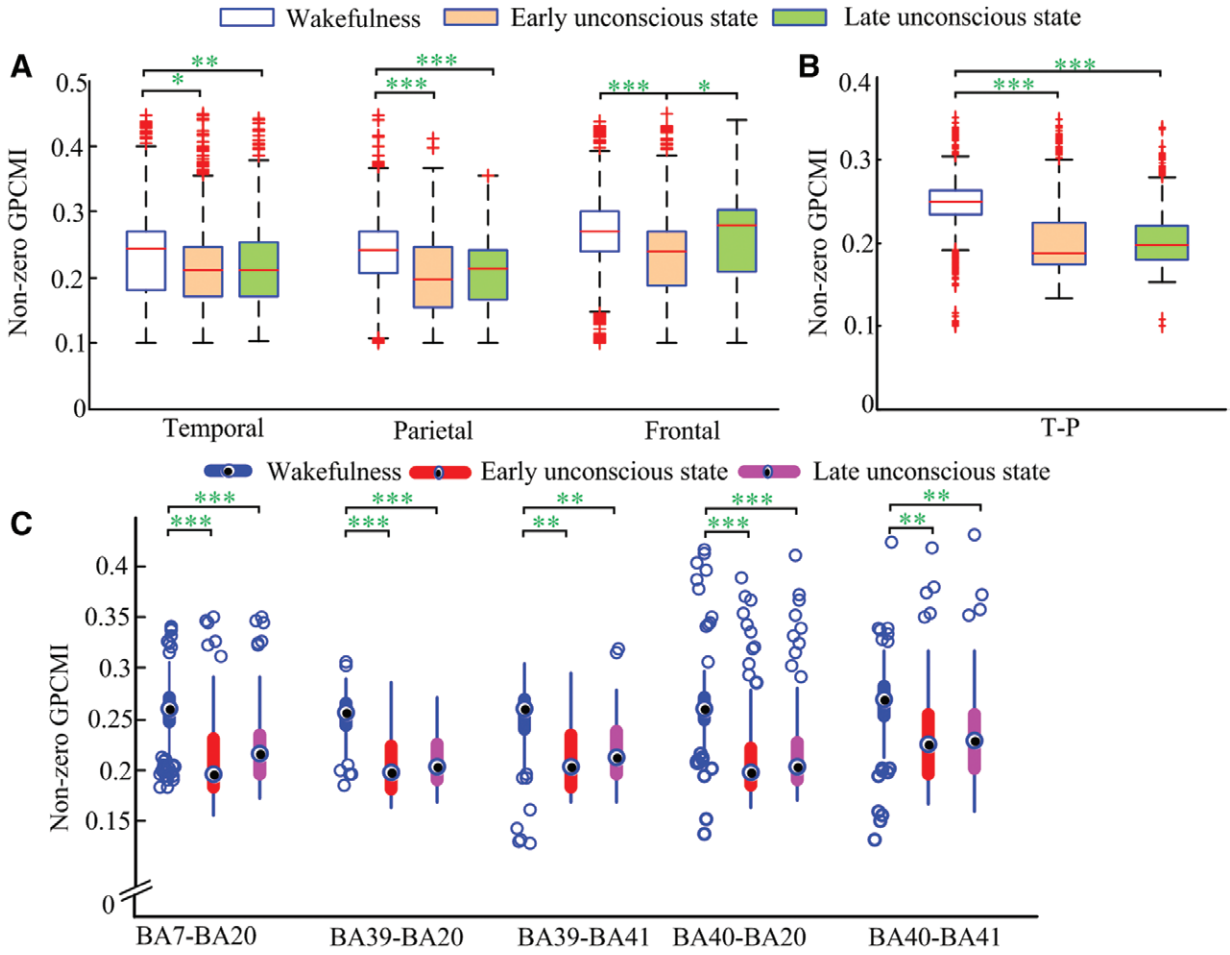

Fig. 6. Nonzero genuine permutation cross mutual information (GPCMI) statistics for intra- and inter-regional information integration in wakefulness, early unconscious state, and late unconscious state. *A* and *B* are the nonzero GPCMI values of intra-region and inter-region electrode pairs, respectively. The *white*, *brown*, and *green* boxes are wakefulness, early unconscious state, and late unconscious state, respectively. T-P, inter-regional information integration between temporal and parietal regions. (*C*) Inter-regional information integration between different Brodmann areas (BA). BA7-BA20 indicates information integration between Brodmann areas 7 and 20. ***Significant difference in the percentage of nonzero GPCMI values at $P < 0.001$ (adjusted by Tukey test).

Generalized linear mixed model analysis showed that the factors of state and Brodmann area for both the nodal clustering coefficient and nodal efficiency indices have interaction effects, $F(12, 839.04) = 4.96$, $P < 0.001$, and $F(12, 842.12) = 3.06$, $P < 0.001$. In every Brodmann area we analyzed, all nodal clustering coefficient values in the wakeful state were significantly higher than those in early unconscious state (primary motor cortex: 0.038 [0.028, 0.049], $P < 0.001$, $d = 0.159$; premotor cortex and supplementary motor cortex: 0.017 [0.010, 0.023], $P < 0.001$, $d = 0.069$; visuo-motor coordination: 0.034 [0.028, 0.041], $P < 0.001$, $d = 0.142$; temporal gyrus: 0.025 [0.019, 0.031], $P < 0.001$, $d = 0.104$; angular gyrus: 0.025 [0.017, 0.032], $P < 0.001$, $d = 0.104$; supramarginal gyrus: 0.027 [0.019, 0.033], $P < 0.001$, $d = 0.112$; auditory cortex: 0.036 [0.031, 0.042], $P < 0.001$, $d = 0.152$), and late unconscious state (primary motor cortex: 0.032 [0.020, 0.045], $P < 0.001$, $d = 0.134$; premotor cortex and supplementary motor cortex: 0.019 [0.012, 0.027], $P < 0.001$, $d = 0.08$; visuo-motor coordination: 0.039 [0.034, 0.044], $P < 0.001$, $d = 0.163$; temporal gyrus: 0.031 [0.024, 0.037], $P < 0.001$, $d = 0.128$; angular gyrus: 0.029 [0.021, 0.036], $P < 0.001$, $d = 0.119$; supramarginal gyrus:0.029 [0.022, 0.036], $P < 0.001$, $d = 0.119$; auditory cortex: 0.041 [0.034, 0.047], $P < 0.001$, $d = 0.168$).There were no significant differences between early and late unconscious states for nodal clustering coefficient in all cortical regions we analyzed (all P values are more than 0.05, *post hoc* comparison with Tukey test). Nodal efficiency indices had similar significance patterns as nodal clustering coefficients. The decrease in nodal clustering coefficients from wakeful to unconscious state indicates a decrease in the connection between each node and its neighbors. Also, the

Table 3. The Statistics of Intra- and Inter-regional Connection of Nonzero Genuine Permutation Cross Mutual Information with Different Cortical Area in Wakefulness and Early Unconscious State and Late Unconscious State

Cortical Area	Wakefulness Median (1st, 3rd quartile) (no.)	Early Unconscious State Median (1st, 3rd quartile) (no.)	Late Unconscious State Median (1st, 3rd quartile) (no.)
Temporal region	0.24 (0.18, 0.27) (n = 1,154)	0.21 (0.17, 0.25) (n = 1,154)	0.21 (0.17, 0.25) (n = 1,146)
Parietal region	0.24 (0.21, 0.27) (n = 1,648)	0.20 (0.16, 0.25) (n = 1,648)	0.21 (0.17, 0.24) (n = 1,018)
Frontal region	0.27 (0.24, 0.30) (n = 1,068)	0.24 (0.19, 0.27) (n = 1,068)	0.28 (0.21, 0.30) (n = 878)
T-P	0.25 (0.23, 0.26) (n = 1,205)	0.19 (0.17, 0.22) (n = 1,205)	0.20 (0.18, 0.22) (n = 989)
BA7-BA20	0.27 (0.25, 0.27) (n = 444)	0.20 (0.18, 0.23) (n = 444)	0.22 (0.20, 0.24) (n = 444)
BA39-BA20	0.26 (0.24, 0.27) (n = 226)	0.20 (0.18, 0.22) (n = 226)	0.20 (0.19, 0.23) (n = 226)
BA39-BA41	0.26 (0.24, 0.27) (n = 94)	0.20 (0.18, 0.24) (n = 94)	0.21 (0.20, 0.24) (n = 94)
BA40-BA20	0.26 (0.25, 0.27) (n = 281)	0.20 (0.18, 0.22) (n = 281)	0.20 (0.19, 0.23) (n = 281)
BA40-BA41	0.27 (0.25, 0.28) (n = 122)	0.23 (0.20, 0.25) (n = 122)	0.23 (0.20, 0.25) (n = 122)

BA, Brodmann area; T-P, between temporal and parietal regions.

decrease in nodal efficiency indices in each node indicates that information exchange efficiency with other nodes decreased. The median (first quartile, third quartile) of the nodal clustering coefficient and nodal efficiency indices in each Brodmann area are presented in tables 4 and 5, respectively.

The multiple comparison tests of the difference among different Brodmann areas in wakefulness and early and late unconscious states are shown in Supplemental Digital Content 6 (http://links.lww.com/ALN/C75). The nodal clustering coefficients for some areas show significant differences from others in wakefulness, for example, primary motor cortex *versus* premotor cortex and supplementary motor cortex and primary motor cortex *versus* temporal gyrus. However, there were no significant differences between these Brodmann areas in early and late unconscious states. This means that the dynamic cortical connectivity was broadly suppressed during propofol anesthesia. Also, the characteristics of nodal clustering coefficient and nodal efficiency within Brodmann areas were inconsistent (*i.e.*, the cortical network characteristics were diverse for different nodes). However, the effect size values for nodal clustering coefficients and nodal efficiency between different cortical regions in different states were relatively small (less than 0.1). The spatial distributions of the nodal clustering coefficients for eight patients in wakefulness and unconscious states are shown in figure 8A and 8B, respectively. For most, the nodal cluster coefficients decreased after loss of consciousness, yet there are some spatial differences.

Lee *et al.*[27] investigated global network changes during propofol-induced anesthesia at the macro scale. To do a matching comparative study, we analyzed the similar global network properties of normalized average clustering coefficient (C_{ave}/C_r), normalized average path length (L_{ave}/L_r), and small worldness (σ) at the mesoscale. Since the average

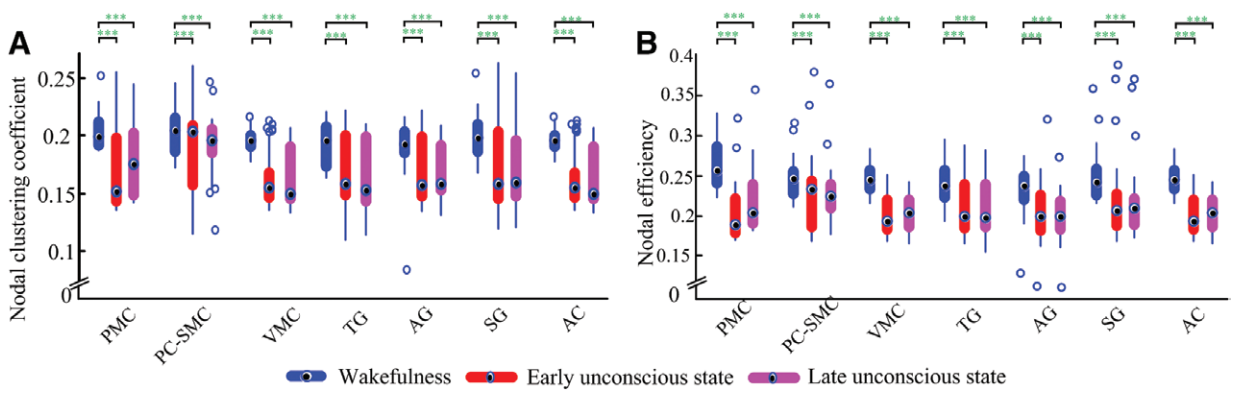

Fig. 7. Compact format boxplots of nodal clustering coefficient (*A*) and nodal efficiency (*B*) for wakefulness (*blue box*), early unconscious state (*red box*), and late unconscious state (*magenta box*) in PMC, PC-SMC, VMC, TG, AG, SG, and AC regions. Box plots show the median value, interquartile range, extremes, and outliers (*blue circles*). ***Significant difference in the percentage of nonzero genuine permutation cross mutual information values at $P < 0.001$. AC, auditory cortex; AG, angular gyrus; PC-SMC, premotor cortex and supplementary motor cortex; PMC, primary motor cortex; SG, supramarginal gyrus; TG, temporal gyrus; VMC, visuo-motor coordination.

Table 4. The Statistics of Nodal Clustering Coefficients with Different Cortical Area in Wakefulness and Early Unconscious State and Late Unconscious State

Cortical Area	Wakefulness Median (1st, 3rd quartile) (no.)	Early Unconscious State Median (1st, 3rd quartile) (no.)	Late Unconscious State Median (1st, 3rd quartile) (no.)
Primary motor cortex	0.20 (0.19, 0.21) (n = 22)	0.15 (0.14, 0.20) (n = 22)	0.18 (0.15, 0.20) (n = 22)
PC-SMC	0.20 (0.19, 0.22) (n = 42)	0.20 (0.16, 0.21) (n = 42)	0.20 (0.19, 0.21) (n = 42)
VMC	0.20 (0.19, 0.20) (n = 66)	0.15 (0.15, 0.17) (n = 66)	0.15 (0.15, 0.19) (n = 66)
Temporal gyrus	0.20 (0.17, 0.21) (n = 48)	0.16 (0.15, 0.20) (n = 48)	0.15 (0.14, 0.20) (n = 48)
Angular gyrus	0.19 (0.19, 0.20) (n = 34)	0.16 (0.15, 0.20) (n = 34)	0.16 (0.15, 0.19) (n = 34)
Supramarginal gyrus	0.20 (0.19, 0.21) (n = 41)	0.16 (0.14, 0.20) (n = 41)	0.16 (0.15, 0.20) (n = 41)
Auditory cortex	0.20 (0.19, 0.20) (n = 66)	0.16 (0.15, 0.17) (n = 66)	0.15 (0.15, 0.19) (n = 66)

PC-SMC, premotor cortex and supplementary motor cortex; VMC, visuo-motor coordination.

Table 5. The Statistics of Nodal Efficiency with Different Cortical Area in Wakefulness and Early Unconscious State and Late Unconscious State

Cortical Area	Wakefulness Median (1st, 3rd quartile) (no.)	Early Unconscious State Median (1st, 3rd quartile) (no.)	Late Unconscious State Median (1st, 3rd quartile) (no.)
Primary motor cortex	0.26 (0.24, 0.29) (n = 22)	0.19 (0.18, 0.22) (n = 22)	0.20 (0.19, 0.24) (n = 22)
PC-SMC	0.25 (0.23, 0.26) (n = 42)	0.23 (0.19, 0.24) (n = 42)	0.22 (0.21, 0.24) (n = 42)
VMC	0.25 (0.23, 0.26) (n = 66)	0.19 (0.18, 0.22) (n = 66)	0.20 (0.19, 0.22) (n = 66)
Temporal gyrus	0.24 (0.22, 0.26) (n = 48)	0.20 (0.19, 0.24) (n = 48)	0.20 (0.19, 0.24) (n = 48)
Angular gyrus	0.24 (0.22, 0.25) (n = 34)	0.20 (0.18, 0.23) (n = 34)	0.20 (0.18, 0.22) (n = 34)
Supramarginal gyrus	0.24 (0.23, 0.26) (n = 41)	0.21 (0.19, 0.23) (n = 41)	0.21 (0.19, 0.22) (n = 41)
Auditory cortex	0.24 (0.23, 0.26) (n = 66)	0.19 (0.18, 0.22) (n = 66)	0.20 (0.19, 0.22) (n = 66)

PC-SMC, premotor cortex and supplementary motor cortex; VMC, visuo-motor coordination.

clustering coefficient (C_{ave}) is the mean of all nodal clustering coefficients, the average clustering coefficients likewise decreased after loss of consciousness. The average path length (L_{ave}) is the inverse of the nodal efficiency for all nodes. Figure 9A shows the evolution of C_{ave}/C_r and L_{ave}/L_r during the time course of propofol-induced anesthesia for one patient. Both the normalized average clustering coefficient and the normalized average path length increased after loss of consciousness in early unconscious state. The statistics for C_{ave}/C_r, L_{ave}/L_r and σ for patients in wakeful and unconscious states (early and late) are shown in figure 9B, 9C, and 9D, respectively. The C_{ave}/C_r and L_{ave}/L_r increased after loss of consciousness in early unconscious state and decreased slightly in late unconscious state, compared with early unconscious state, $F(2,7) = 7.96$, $P = 0.033$; $F(2,7) = 8.19$, $P = 0.027$). The significant increases in L_{ave}/L_r in early unconscious state (1.02 ± 0.01 [mean ± SD] *versus* 1.04 ± 0.01, $P = 0.021$) suggest that the cortical network lost some global information transmission capacity after loss of consciousness. Increased C_{ave}/C_r (1.05 ± 0.01 *versus* 1.06 ± 0.03, $P = 0.037$) reflects an increase in local functional segregation. The decreases of these two indices in late conscious state, compared with early unconscious, indicate that brain networks changed when the propofol concentration decreased. Figure 9D shows that all cortical networks in wakefulness and unconsciousness had the small worldness property ($\sigma > 1$ and L_{ave}/L_r approximately 1). However, there was no significant difference between these three states, $F(2,7) = 4.16$, $P = 0.478$). These results are similar to those seen from scalp electroencephalogram data reported in the study of Lee *et al.*[27] This suggests that propofol disrupts efficient network structures on the mesoscale. The increase and decrease in these indices in early and late unconscious states may be related to drug concentration changes after loss of consciousness.

Discussion

This study investigated cortical information integration during propofol-induced loss of consciousness (loss of consciousness) at mesoscale. We analyzed the genuine permutation cross mutual information between electrodes with different separation distances in different brain areas, and with local and global network metrics. The results suggested that cortical information coupling and network connections at the mesoscopic level were correlated with electrode distances and particular to each brain area. Also,

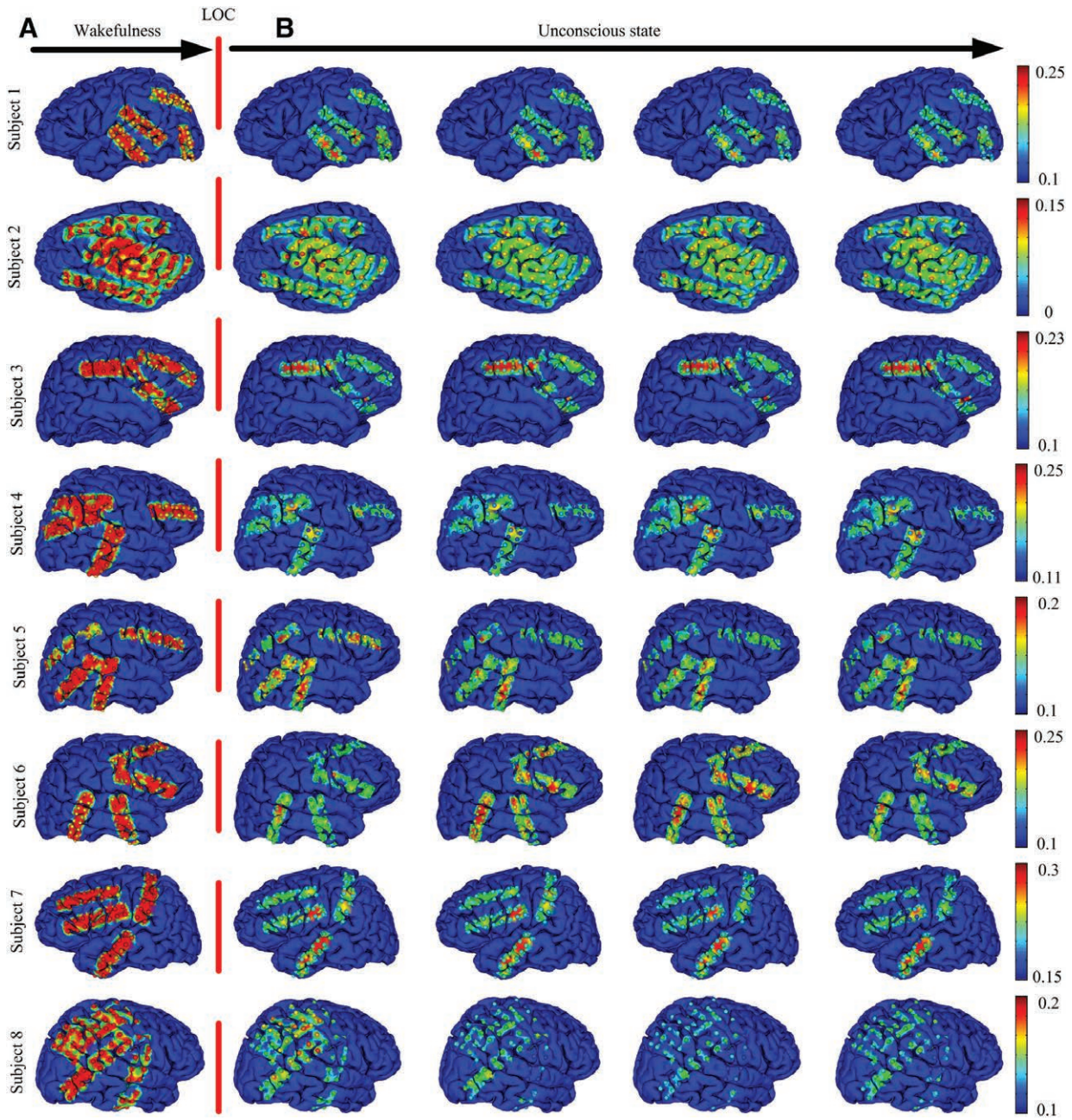

Fig. 8. Spatial distributions of generalized linear mixed model indices for eight patients in wakefulness (A) and unconscious states (B). LOC, loss of consciousness.

the information integration capacity in the cortical network was inhibited by propofol. The findings are summarized as follows:

(1) The genuine permutation cross mutual information decreased uniformly from narrow to wide electrode separation. For wakeful and unconscious states, nonzero genuine permutation cross mutual information values decreased as the linear surface distance increased, up to a maximum of about 3 cm. This suggests that information integration strength is related to the separation distance, and there is a floor effect for distances greater than 3 cm.

(2) The proportion of nonzero genuine permutation cross mutual information values decreased along with increasing distance in wakeful and unconscious states; the proportion of nonzero values was smaller in the unconscious states than in wakefulness. This indicates that communication capacity decreased as distance increased.

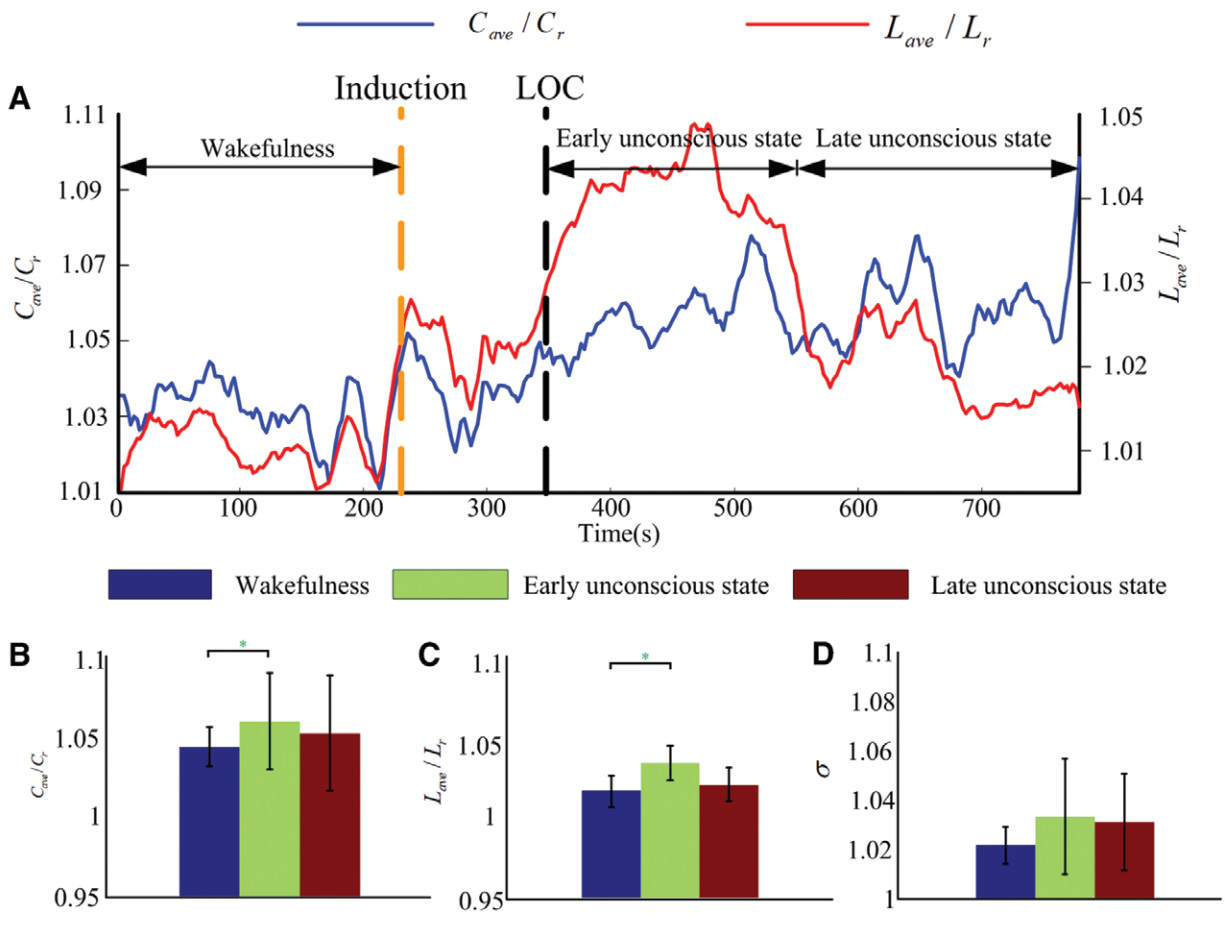

Fig. 9. Analysis of the global network parameters normalized average clustering coefficient (C_{ave}/C_r) and normalized average path length (L_{ave}/L_r). (*A*) C_{ave}/C_r (*blue curve*) and L_{ave}/L_r (*red curve*) of one patient (same as in fig. 3). (*B* through *D*) Statistics for C_{ave}/C_r, L_{ave}/L_r, σ for all patients in wakefulness, early unconscious state, and late unconscious state. *Significant difference of the indices at $P < 0.05$. LOC, loss of consciousness.

(3) The nodal clustering coefficient and nodal efficiency values of different Brodmann areas significantly decreased after loss of consciousness ($P < 0.001$). This indicates that nodal-to-neighbor connection decreased and communication efficiency of the local network also decreased after loss of consciousness.

(4) The global network properties of normalized average clustering coefficient and normalized average path length increased in early unconscious state. This reflects the enhancement of local functional segregation and inefficient global information transmission after propofol-induced anesthesia at cortical scale.

Genuine Permutation Cross Mutual Information Measurement Can Distinguish States of Consciousness

Genuine permutation cross mutual information-based cortical network analysis has several advantages. First, as a nonlinear analysis method, it combines a symbolic dynamics measure and information theory. Thus, this measure can examine the nonlinear characteristics in electrocorticogram time series. Antinoise capability and sensitivity to changes in coupling strength have been evaluated in our previous works.[7,47] In this study, we also modeled and evaluated the effectiveness of genuine permutation cross mutual information in the presence of epileptiform spiking (see Supplemental Digital Content 2, http://links.lww.com/ALN/C71). Genuine permutation cross mutual information is a significance-testable connection measure based on surrogate analysis and the Wilcoxon signed-rank test, thus it can mitigate the confounding impact of low frequency oscillations and finite size datasets.[24] Finally, genuine cortical networks built using genuine permutation cross mutual information can be analyzed using graph theory metrics, which can characterize the cortical functional connectivity derived from information theory.

Various measures and theories have been proposed to interpret anesthesia-induced loss of consciousness. Mashour proposed the "cognitive unbinding" theory which suggests that it is the impaired synthesis of cognitive activities that drives the mechanism of loss of consciousness in anesthesia.[50] In particular, the disruption of spatio-temporal synchronization and convergence are the fundamental principles of the cognitive unbinding paradigm.[50] In support of these hypotheses, Lee *et al.*[51] used the mean information integration measure to analyze the mechanism of propofol induced unconsciousness, and Jordan *et al.*[52] analyzed the directional connectivity in electroencephalogram signals during propofol anesthesia—based on symbolic transfer entropy—and compared with the functional brain imaging connectivity. In recent years, a similar mutual information measure, weighted symbolic mutual information, has been proposed to reflect different states of consciousness (vegetative states, minimally conscious states, and conscious states).[15,53,54] The advantage of the weighted symbolic mutual information is that it can eliminate the influence of volume conduction effects. These studies suggest that the symbolic dynamics-based information integration theory is a powerful tool for measuring consciousness.

Information Integration Capacity Is Correlated with the Linear Surface Distance at the Cortical Scale

The nonzero genuine permutation cross mutual information values at different linear surface distances revealed that integration strength of two electrodes significantly decreased with increasing distance, especially for distances less than 3 cm. Lewis *et al.*[55] also investigated propofol-induced unconsciousness based on electrocorticogram data. They reported that the phase-locking factor magnitude dropped significantly with distance, especially for long distances (greater than 4 cm). This finding used different methods, but it is consistent with our analysis based on genuine permutation cross mutual information measures, and corroborated our results. King *et al.*[15] have also investigated weighted symbolic mutual information changes in pairs of channels as distance increased at the electroencephalogram scale. They found that weighted symbolic mutual information decreased along with increases in inter-channel distance. Although the distances they measured ranged from 6.3 to 21.8 cm (quite different from the electrocorticogram data in our study), information integration capacity decreased with increasing separation. This is likely an important phenomenon of brain conscious processing.

Propofol Disrupts Efficient Information Transmission at Cortical Scales

If general anesthesia is characterized by disrupted network integration, it would be natural to explore the properties of neural activity at the cortical-network-level when investigating anesthetic state transitions.[24] Graph theory is an attractive method for analyzing the brain's functional networks.[35] In our study, the increased normalized average path length and clustering coefficient during unconsciousness support the hypothesis that disruption of the normal integration of global neural information may induce loss of consciousness. Significant changes in local networks and integration information disruption have also been found for propofol and isoflurane in an electroencephalogram study,[27] and also in magnetic resonance imaging studies.[56,57] We observed a similar significant decline in long-distance connections (nonzero genuine permutation cross mutual information values decreased as distance increased) and a reduction in cortical spatiotemporal integration (decreased genuine permutation cross mutual information and increased normalized average path length after loss of consciousness). This observation is consistent with a topologic reconfiguration during propofol-induced loss of consciousness.

However, from the perspective of clinical care, because of the incomplete understanding of consciousness, an ideal monitor for the brain during surgery is still lacking.[58,59] Locating a state-specific biomarker may promote the construction of agent-related signatures that would be helpful for monitoring brain states during perioperative periods. In addition to supplementing the insufficient understanding of neural-correlated consciousness on the mesoscale, our findings also provide a potential clinical tool based on connectivity and network structure analysis.

Volume Conduction Is a Nonnegligible Factor in Electrocorticogram Analysis

We found that permutation cross mutual information was higher for close-by channels in the raw electrocorticogram, and the linear correlation values of these close-by channels pairs were higher than those distant channel pairs, in wakefulness and unconscious states (fig. S11 in Supplemental Digital Content 2, http://links.lww.com/ALN/C71). Studies have proposed that the volume conduction effect may be the cause of the observed high linear correlation seen in close electrodes pairs in electrocorticogram data.[38–40] We used independent component analysis to reduce the effect of volume conduction, and compared it with the current source density transform.[60] The results showed that the square Pearson correlation decreased after the independent component analysis based procedure, whereas it increased after the current source density transform (fig. S20 in Supplemental Digital Content 2, http://links.lww.com/ALN/C71). This suggests that volume conduction effects cannot be ignored in electrocorticogram signal analysis. Volume conduction is a function of the physical tissue characteristics, and it is hard to see how these physical characteristics could be altered with propofol anesthesia; but we might speculate that the drug is having this effect by altering neuronal polarization. Based on our results, we believe that independent component analysis–based processing works better than current source density transform for removing volume conduction in electrocorticogram signals.

Limitations of This Study

Similar to the studies of Breshears *et al.*[19] and Lewis *et al.*,[55] electrocorticogram signals were recorded from epileptic patients. The same limitations which were addressed in these works also existed in our study. First, the electrode coverage was determined by clinical criteria. Therefore, the findings of the present study can only be interpreted in the context of the covered cortical areas. Also, the electrodes' resolution was 1 cm. Therefore, the information integration between cortical areas separated by less than 1 cm could not be measured. Second, a detailed dosage timeline was not recorded during the administration of anesthesia. Thus, effect-site concentrations could not be estimated. The electrocorticogram signals were only recorded from wakefulness to unconscious states, so we could not compare the differences between the loss of consciousness and the recovery of consciousness. Third, Breshears *et al.*[19] pointed out that the electrocorticogram may differ between epileptic patients and the healthy population because of the effect of seizure foci and antiepileptic drug therapy. Whether the findings of this study can be generalized to the healthy brain requires additional in-depth investigation. Finally, despite the significant differences in genuine permutation cross mutual information measures over different electrode distances—seen even with a small sample size and unbalanced number of electrodes in each cortical region—we cannot extrapolate our findings to a broad population and to other anesthetics, such as volatile anesthetics and opioids. This study is a relatively small size and so is reliant on surrogate analysis techniques to obtain reliable correlation values from the electrocorticogram recordings. To validate the hypothesis, further research and analysis are necessary through the multi-hospital or multi-center cooperation.

Conclusions

This study found that, at the mesoscale level, propofol-induced loss of consciousness is associated with a reduction in information integration and a concomitant decrease in network complexity—consistent with scalp electroencephalogram studies. Our findings shed light on the functional significance of neural activity as measured by electrocorticogram signals. They also bridge the gap between the micro (local field potential) and the macro (electroencephalogram) level in understanding propofol-induced loss of consciousness.

Acknowledgments

The authors thank Yang Bai, Ph.D., from the Department of Basic Medical Science, School of Medicine, Hangzhou Normal University, Hangzhou, China, for statistical computing support.

Research Support

This study was supported by National Natural Science Foundation of China grant No. 81230023 (Beijing, China; to Dr. Li) and grant No. 61673333 (to Dr. Liang).

Competing Interests

The authors declare no competing interests.

Correspondence

Address correspondence to Dr. Li: State Key Laboratory of Cognitive Neuroscience and Learning and International Data Group/McGovern Institute for Brain Research, Beijing Normal University, Beijing 100875, P.R. China, 010-58802032. xiaoli@bnu.edu.cn.

References

1. Varela F, Lachaux JP, Rodriguez E, Martinerie J: The brainweb: Phase synchronization and large-scale integration. Nat Rev Neurosci 2001; 2:229–39
2. Jacobs J, Kahana MJ: Direct brain recordings fuel advances in cognitive electrophysiology. Trends Cogn Sci 2010; 14:162–71
3. Tononi G, Sporns O: Measuring information integration. BMC Neurosci 2003; 4:31
4. Andrzejak RG, Schindler K, Rummel C: Nonrandomness, nonlinear dependence, and nonstationarity of electroencephalographic recordings from epilepsy patients. Phys Rev E Stat Nonlin Soft Matter Phys 2012; 86(4 Pt 2):046206
5. Sarasso S, Boly M, Napolitani M, Gosseries O, Charland-Verville V, Casarotto S, Rosanova M, Casali AG, Brichant JF, Boveroux P, Rex S, Tononi G, Laureys S, Massimini M: Consciousness and complexity during unresponsiveness induced by propofol, xenon, and ketamine. Curr Biol 2015; 25:3099–105
6. Thul A, Lechinger J, Donis J, Michitsch G, Pichler G, Kochs EF, Jordan D, Ilg R, Schabus M: EEG entropy measures indicate decrease of cortical information processing in disorders of consciousness. Clin Neurophysiol 2016; 127:1419–27
7. Liang Z, Ren Y, Yan J, Li D, Voss LJ, Sleigh JW, Li X: A comparison of different synchronization measures in electroencephalogram during propofol anesthesia. J Clin Monit Comput 2016; 30:451–66
8. Lee U, Blain-Moraes S, Mashour GA: Assessing levels of consciousness with symbolic analysis. Philos Trans A Math Phys Eng Sci 2015; 373
9. Bandt C, Pompe B: Permutation entropy: A natural complexity measure for time series. Phys Rev Lett 2002; 88:174102
10. Martin MT, Plastino A, Rosso OA: Generalized statistical complexity measures: Geometrical and analytical properties. Physica. Section A 2006: 439-62

11. Amigo JM, Keller K, Unakafova VA: Ordinal symbolic analysis and its application to biomedical recordings. Philos Trans A Math Phys Eng Sci 2015; 373
12. Zunino L, Olivares F, Rosso OA: Permutation min-entropy: An improved quantifier for unveiling subtle temporal correlations. Epl 2015; 109: 10005
13. Martini M, Kranz TA, Wagner T, Lehnertz K: Inferring directional interactions from transient signals with symbolic transfer entropy. Phys Rev E Stat Nonlin Soft Matter Phys 2011; 83(1 Pt 1):011919
14. Ferlazzo E, Mammone N, Cianci V, Gasparini S, Gambardella A, Labate A, Latella MA, Sofia V, Elia M, Morabito FC, Aguglia U: Permutation entropy of scalp EEG: A tool to investigate epilepsies: Suggestions from absence epilepsies. Clin Neurophysiol 2014; 125:13–20
15. King JR, Sitt JD, Faugeras F, Rohaut B, El Karoui I, Cohen L, Naccache L, Dehaene S: Information sharing in the brain indexes consciousness in noncommunicative patients. Curr Biol 2013; 23:1914–9
16. Liang Z, Liang S, Wang Y, Ouyang G, Li X: Tracking the coupling of two electroencephalogram series in the isoflurane and remifentanil anesthesia. Clin Neurophysiol 2015; 126:412–22
17. Li D, Li X, Liang Z, Voss LJ, Sleigh JW: Multiscale permutation entropy analysis of EEG recordings during sevoflurane anesthesia. J Neural Eng 2010; 7:046010
18. Olofsen E, Sleigh JW, Dahan A: Permutation entropy of the electroencephalogram: A measure of anaesthetic drug effect. Br J Anaesth 2008; 101:810–21
19. Breshears JD, Roland JL, Sharma M, Gaona CM, Freudenburg ZV, Tempelhoff R, Avidan MS, Leuthardt EC: Stable and dynamic cortical electrophysiology of induction and emergence with propofol anesthesia. Proc Natl Acad Sci USA 2010; 107:21170–5
20. Baars BJ: Global workspace theory of consciousness: Toward a cognitive neuroscience of human experience. Prog Brain Res 2005; 150:45–53
21. Dehaene S, Changeux JP: Experimental and theoretical approaches to conscious processing. Neuron 2011; 70:200–27
22. Bola M, Barrett AB, Pigorini A, Nobili L, Seth AK, Marchewka A: Loss of consciousness is related to hyper-correlated gamma-band activity in anesthetized macaques and sleeping humans. Neuroimage 2018; 167:130–42
23. Müller M, Baier G, Rummel C, Schindler K: Estimating the strength of genuine and random correlations in non-stationary multivariate time series. Epl 2008; 84: 10009
24. Lee U, Müller M, Noh GJ, Choi B, Mashour GA: Dissociable network properties of anesthetic state transitions. Anesthesiology 2011; 114:872–81
25. Rembado I, Castagnola E, Turella L, Ius T, Budai R, Ansaldo A, Angotzi GN, Debertoldi F, Ricci D, Skrap M, Fadiga L: Independent component decomposition of human somatosensory evoked potentials recorded by micro-electrocorticography. Int J Neural Syst 2017; 27:1650052
26. Whitmer D, Worrell G, Stead M, Lee IK, Makeig S: Utility of independent component analysis for interpretation of intracranial EEG. Front Hum Neurosci 2010; 4:184
27. Lee H, Mashour GA, Noh GJ, Kim S, Lee U: Reconfiguration of network hub structure after propofol-induced unconsciousness. Anesthesiology 2013; 119:1347–59
28. Schreiber T, Schmitz A: Improved surrogate data for nonlinearity tests. Phys Rev Lett 1996; 77:635–8
29. Hilger K, Ekman M, Fiebach CJ, Basten U: Efficient hubs in the intelligent brain: Nodal efficiency of hub regions in the salience network is associated with general intelligence. Intelligence 2017; 60: 10–25
30. Bullmore E, Sporns O: Complex brain networks: graph theoretical analysis of structural and functional systems. Nat Rev Neurosci 2009; 10:186–98
31. Stam CJ: Modern network science of neurological disorders. Nat Rev Neurosci 2014; 15:683–95
32. Stam CJ, de Haan W, Daffertshofer A, Jones BF, Manshanden I, van Cappellen van Walsum AM, Montez T, Verbunt JP, de Munck JC, van Dijk BW, Berendse HW, Scheltens P: Graph theoretical analysis of magnetoencephalographic functional connectivity in Alzheimer's disease. Brain 2009; 132(Pt 1):213–24
33. Cai L, Dong Q, Niu H: The development of functional network organization in early childhood and early adolescence: A resting-state fNIRS study. Dev Cogn Neurosci 2018; 30:223–35
34. Latora V, Marchiori M: Efficient behavior of small-world networks. Phys Rev Lett 2001; 87:198701
35. Rubinov M, Sporns O: Complex network measures of brain connectivity: Uses and interpretations. Neuroimage 2010; 52:1059–69
36. Maslov S, Sneppen K: Specificity and stability in topology of protein networks. Science 2002; 296:910–3
37. Wang Y, Yan J, Wen J, Yu T, Li X: An intracranial electroencephalography (iEEG) brain function mapping tool with an application to epilepsy surgery evaluation. Front Neuroinform 2016; 10:15
38. Burns SP, Santaniello S, Yaffe RB, Jouny CC, Crone NE, Bergey GK, Anderson WS, Sarma SV: Network dynamics of the brain and influence of the epileptic seizure onset zone. Proc Natl Acad Sci USA 2014; 111:E5321–30
39. Keller CJ, Honey CJ, Megevand P, Entz L, Ulbert I, Mehta AD: Mapping human brain networks with cortico-cortical evoked potentials. Philos Trans R Soc Lond B Biol Sci 2014; 369
40. Collard MJ, Fifer MS, Benz HL, McMullen DP, Wang Y, Milsap GW, Korzeniewska A, Crone NE: Cortical subnetwork dynamics during human language tasks. Neuroimage 2016; 135:261–72

41. Hindriks R, Micheli C, Bosman CA, Oostenveld R, Lewis C, Mantini D, Fries P, Deco G: Source-reconstruction of the sensorimotor network from resting-state macaque electrocorticography. Neuroimage 2018; 181:347–58
42. Fischer F, Pieper F, Galindo-Leon E, Engler G, Hilgetag CC, Engel AK: Intrinsic functional connectivity resembles cortical architecture at various levels of isoflurane anesthesia. Cereb Cortex 2018; 28:2991–3003
43. Watts AD, Herrick IA, McLachlan RS, Craen RA, Gelb AW: The effect of sevoflurane and isoflurane anesthesia on interictal spike activity among patients with refractory epilepsy. Anesth Analg 1999; 89:1275–81
44. Chui J, Manninen P, Valiante T, Venkatraghavan L: The anesthetic considerations of intraoperative electrocorticography during epilepsy surgery. Anesth Analg 2013; 117:479–86
45. Chaitanya G, Arivazhagan A, Sinha S, Reddy KR, Thennarasu K, Bharath RD, Rao MB, Chandramouli BA, Satishchandra P: Dexmedetomidine anesthesia enhances spike generation during intra-operative electrocorticography: A promising adjunct for epilepsy surgery. Epilepsy Res 2015; 109:65–71
46. Brysbaert M, Stevens M: Power analysis and effect size in mixed effects models: A tutorial. J Cogn 2018; 1:9
47. Li X, Ouyang G: Estimating coupling direction between neuronal populations with permutation conditional mutual information. Neuroimage 2010; 52:497–507
48. Khadem A, Hossein-Zadeh GA: Quantification of the effects of volume conduction on the EEG/MEG connectivity estimates: An index of sensitivity to brain interactions. Physiol Meas 2014; 35:2149–64
49. Gugino LD, Chabot RJ, Prichep LS, John ER, Formanek V, Aglio LS: Quantitative EEG changes associated with loss and return of consciousness in healthy adult volunteers anaesthetized with propofol or sevoflurane. Br J Anaesth 2001; 87:421–8
50. Mashour GA: Cognitive unbinding: A neuroscientific paradigm of general anesthesia and related states of unconsciousness. Neurosci Biobehav Rev 2013; 37(10 Pt 2):2751–9
51. Lee U, Mashour GA, Kim S, Noh GJ, Choi BM: Propofol induction reduces the capacity for neural information integration: Implications for the mechanism of consciousness and general anesthesia. Conscious Cogn 2009; 18:56–64
52. Jordan D, Ilg R, Riedl V, Schorer A, Grimberg S, Neufang S, Omerovic A, Berger S, Untergehrer G, Preibisch C, Schulz E, Schuster T, Schröter M, Spoormaker V, Zimmer C, Hemmer B, Wohlschläger A, Kochs EF, Schneider G: Simultaneous electroencephalographic and functional magnetic resonance imaging indicate impaired cortical top-down processing in association with anesthetic-induced unconsciousness. Anesthesiology 2013; 119:1031–42
53. Engemann DA, Raimondo F, King JR, Rohaut B, Louppe G, Faugeras F, Annen J, Cassol H, Gosseries O, Fernandez-Slezak D, Laureys S, Naccache L, Dehaene S, Sitt JD: Robust EEG-based cross-site and cross-protocol classification of states of consciousness. Brain 2018; 141:3179–92
54. Sitt JD, King JR, El Karoui I, Rohaut B, Faugeras F, Gramfort A, Cohen L, Sigman M, Dehaene S, Naccache L: Large scale screening of neural signatures of consciousness in patients in a vegetative or minimally conscious state. Brain 2014; 137(Pt 8):2258–70
55. Lewis LD, Weiner VS, Mukamel EA, Donoghue JA, Eskandar EN, Madsen JR, Anderson WS, Hochberg LR, Cash SS, Brown EN, Purdon PL: Rapid fragmentation of neuronal networks at the onset of propofol-induced unconsciousness. Proc Natl Acad Sci USA 2012; 109:E3377–86
56. Schröter MS, Spoormaker VI, Schorer A, Wohlschläger A, Czisch M, Kochs EF, Zimmer C, Hemmer B, Schneider G, Jordan D, Ilg R: Spatiotemporal reconfiguration of large-scale brain functional networks during propofol-induced loss of consciousness. J Neurosci 2012; 32:12832–40
57. Liang Z, King J, Zhang N: Intrinsic organization of the anesthetized brain. J Neurosci 2012; 32:10183–91
58. Vlisides PE, Li D, Zierau M, Lapointe AP, Ip KI, McKinney AM, Mashour GA: Dynamic cortical connectivity during general anesthesia in surgical patients. Anesthesiology 2019; 130:885–97
59. Li D, Vlisides PE, Kelz MB, Avidan MS, Mashour GA; ReCCognition Study Group: Dynamic cortical connectivity during general anesthesia in healthy volunteers. Anesthesiology 2019; 130:870–84
60. Kayser J, Tenke CE: Principal components analysis of Laplacian waveforms as a generic method for identifying ERP generator patterns: I. Evaluation with auditory oddball tasks. Clin Neurophysiol 2006; 117:348–68